Combined Coal Gasification and Alkaline Water Electrolyzer for Hydrogen Production

by

Munur Sacit Herdem

A thesis
presented to the University of Waterloo
in fulfillment of the
thesis requirement for the degree of
Master of Applied Science
in
Mechanical Engineering

Waterloo, Ontario, Canada, 2013

I hereby declare that I am the sole author of this thesis. This is a true copy of the thesis, including any required final revisions, as accepted by my examiners.

I understand that my thesis may be made electronically available to the public.

Abstract

There have been many studies in the energy field to achieve different goals such as energy security, energy independence and production of cheap energy. The consensus of the general population is that renewable energy sources can be used on a short-term basis to compensate for the energy requirement of the world. However, the prediction is that fossil fuels will be used to provide the majority of energy requirements in the world at least on a short-term basis. Coal is one of the major fossil fuels and will be used for a long time because there are large coal reservoirs in the world and many products such as hydrogen, ammonia, and diesel can be produced using coal.

In the present study, the performance of a clean energy system that combines the coal gasification and alkaline water electrolyzer concepts to produce hydrogen is evaluated through thermodynamic modeling and simulations. A parametric study is conducted to determine the effect of water ratio in coal slurry, gasifier temperature, effectiveness of carbon dioxide removal, and hydrogen recovery efficiency of the pressure swing adsorption unit on the system hydrogen production. In addition, the effects of different types of coals on the hydrogen production are estimated. The exergy efficiency and exergy destruction in each system component are also evaluated. Although this system produces hydrogen from coal, the greenhouse gases emitted from this system are fairly low.

Acknowledgements

I wish to express deep gratitude to my co-supervisors Prof. Feridun Hamdullahpur and Prof. Ibrahim Dincer for their advice and encouragement for this research thesis.

I would like to express sincere thanks to Dr. Siamak Farhad for his invaluable advice, moral support, and insight throughout the research process.

I gratefully acknowledge the financial support provided by Ministry of Education in Turkey. I would also like to appreciate Mr. Dennis Herman and the Chemical Engineering Department at the University of Waterloo for providing Aspen Plus software.

Last, but not least, I thank my mother and my sisters for their invaluable support in my entire life.

To my mother and my sisters…

Table of Contents

List of Figures

List of Tables

List of Symbols

Nomenclature

c_p	Specific heat, kJ/kg.K
ex_{ch}	Specific chemical exergy, kJ/kmol
ex_{ph}	Specific physical exergy, kJ/kg
$\dot{E}x_D$	Exergy destruction rate, kW
ΔG	Gibbs function, kJ/kmol
h	Specific enthalpy, kJ/kg
H	Enthalpy per unit mole, kJ/kmol.K
$\dot{m}_{coal}$	Coal flow rate fed to the gasifier, kg/h
$\dot{m}_{H_2}$	Total hydrogen production rate, kg/h
$\eta_{ex,system}$	Overall exergy efficiency of the system
$\eta_{en,system}$	Overall energy efficiency of the system
R	Universal gas constant, kJ/kmol.K
s	Specific entropy, kJ/kg.K
S	Entropy per unit mole, kJ/kmol.K
T_0	Environmental temperature, K
$\bar{w}$	Work per unit mole, kJ/kmol.K
$\dot{W}$	Work rate, kW
Y_D	Exergy destruction ratio

y_i	Molar fraction of gas species

Acronyms

ASU	Air separation unit
HRSG	Heat recovery steam generator
IGCC	Integrated gasification combined cycle
LHV	Lower heating value
PSA	Pressure swing adsorption
WGS	Water gas shift

Superscripts and subscripts

act	Actual
C	Compressor
CO_2ru	Carbon dioxide removal unit
elec	Electrolysis
F	Fuel
H_2O	Water
in	Inlet
min	Minimum
out	Outlet
rev	Reversible
sep	Separator
T	Turbine
tot	Total

Chapter 1

Introduction

1.1 Energy Demand and Supply

Energy, which is used for heating, cooling, transportation and to produce electricity, is a key factor for human civilization for social and economic development. The world population and the industrial growth in countries have dramatically increased. The prediction is that the world`s population will be from about 7 billion people today to approximately 9 billion people by 2040 [1]. Therefore, the requirement of energy is one of the major concerns in the world and will remain as one of the top – ten global concerns in this century [2]. Figure 1.1 shows the world energy consumption and projection of the energy consumption in 2040. As shown in the figure, although global energy consumption was about 350 quadrillion Btu in 1990, it expanded approximately 520 quadrillion Btu in 2010, and it is predicted that world energy consumption will be about 810 quadrillion Btu in 2040 [3].

Currently, many researches are being accomplished in the field of energy to achieve solutions for sustainable production of large amount of energy with low cost and minimum negative impacts on the environment. In addition, solutions for energy security, energy independence and production of cheap energy are currently being researched. Development and using renewable energy sources is one of these solutions. There are some recent studies about large – scale development of renewable energy to provide energy requirement of the U.S [4], UK [5], Australia [6], Europe [7, 8], and the world [9]. The idea in these studies is that renewable energy sources can be used to provide all of the energy requirement in these countries, regions

and the world in intermediate terms. However, difficulties in production of large amounts of electricity using renewable energy sources such as solar, wind, and geothermal as well as their investment cost and availability are important issues of renewable energy sources [10]. It seems that fossil fuels will remain as the major energy sources, for the near future. The world energy demand has been predicted by many organizations such as U.S Energy Information Administration (EIA) [3], the International Energy Agency (IEA) [11], and the Organization of the Petroleum Exporting Countries (OPEC) [12]. Although there are some different backgrounds and assumptions in these outlooks [13], the accepted vision is that using fossil fuels to compensate world energy demand will continue to grow in the future.

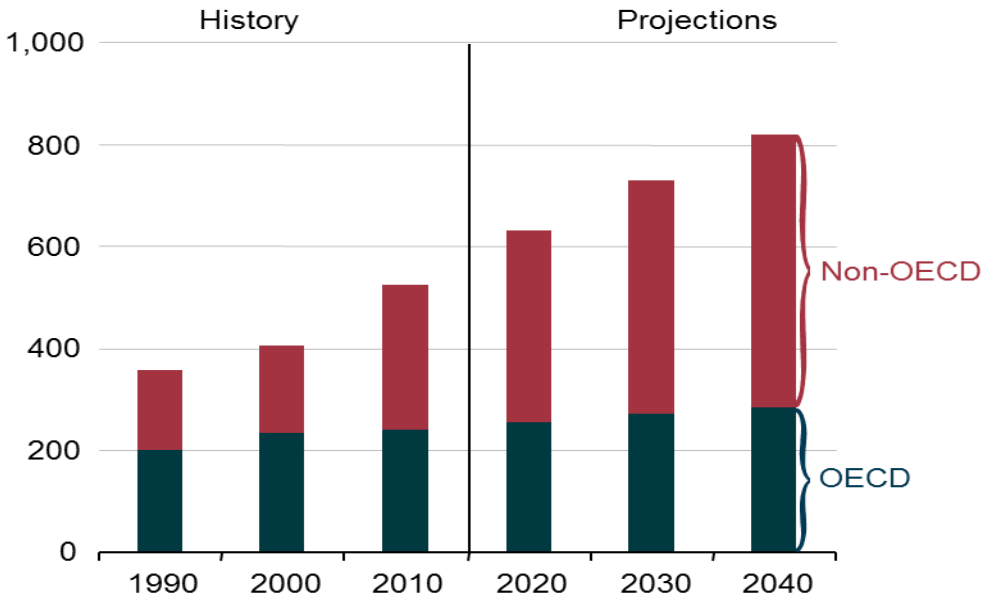

Figure 1.1: World energy consumption, 1990-2040 (quadrillion Btu) (Adapted from [3])

World energy consumption by fuel type, from 1990 to 2040 is shown in Figure 1.2. As can be seen in figure 1.2, renewable energy and nuclear power are the fastest – growing energy sources; however, majority of the global energy demand- more than 80% will be supplied from fossil fuels through 2040. In addition, after the Fukushima Daiichi nuclear power plants accident, many countries changed in nuclear policies, so it will significantly affect future fossil fuel demand in the world [13].

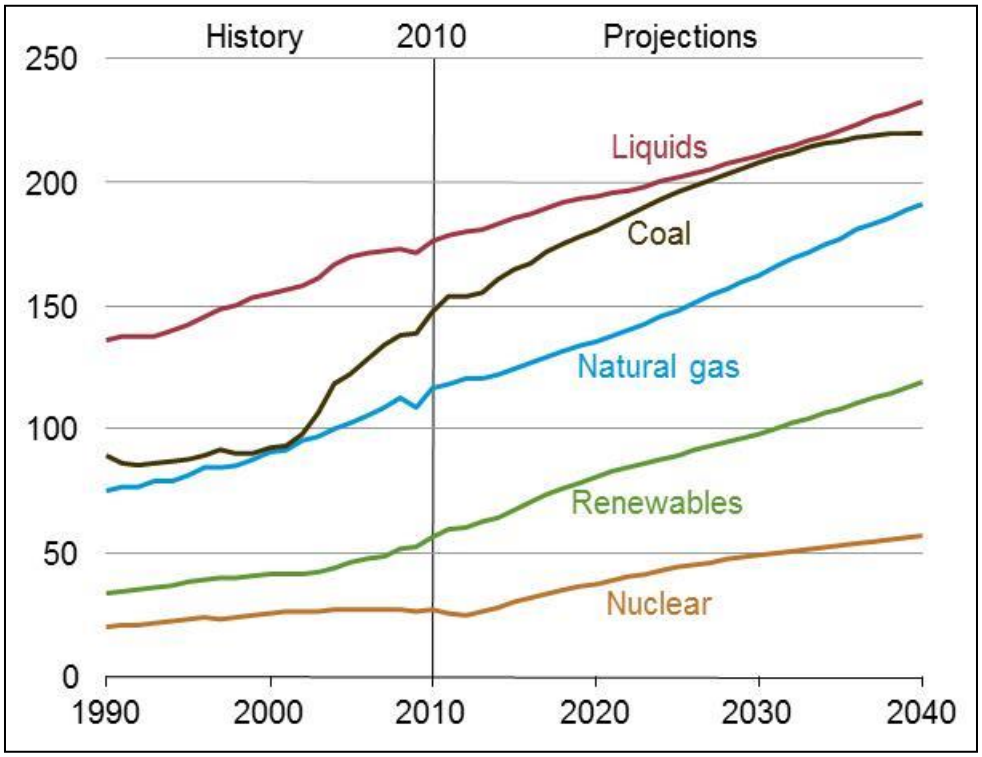

Figure 1.2: World energy consumption by fuel type, for 1990 – 2040 (quadrillion Btu) (Adapted from [3])

Coal is one of the major fossil fuels and can be used for a long time due to the large coal reservoirs in the world. According to World Coal Association estimation, there are more than

861 billion tons of proven coal reserves in the world [14]. In particular, large amounts of electricity in the world is produced from coal, and it is estimated that about 35% of the electricity production will be from coal in 2040 [3].

Although coal is usually employed to produce power, it may have serious negative impacts on the environment. Of course, the coal gasification system is a promising technology to produce electricity and fuel with minimum adverse impact on the environment because this technology has a potential for carbon capturing.

1.2 Hydrogen Production

Hydrogen can be used as an energy carrier (not an energy source) in the future. To provide energy for the increasing global demand because it does not have any negative impacts on the environment and can be obtained by using primary energy sources. Since hydrogen is not available naturally, the main challenge with using hydrogen is the production of it. Hydrogen can be produced by using fossil fuels such as coal, petroleum, natural gas; renewable energy sources, such as hydroelectric power, wind power systems, biomass production, photovoltaic energy conversion, and nuclear energy [15]. Currently, about 50% of the hydrogen is produced via steam reforming of natural gas, approximately 30% from oil/naphtha reforming from refinery/chemical industrial off-gases, 18% from coal gasification, 3.9% from water electrolysis and 0.1% from other sources [16].

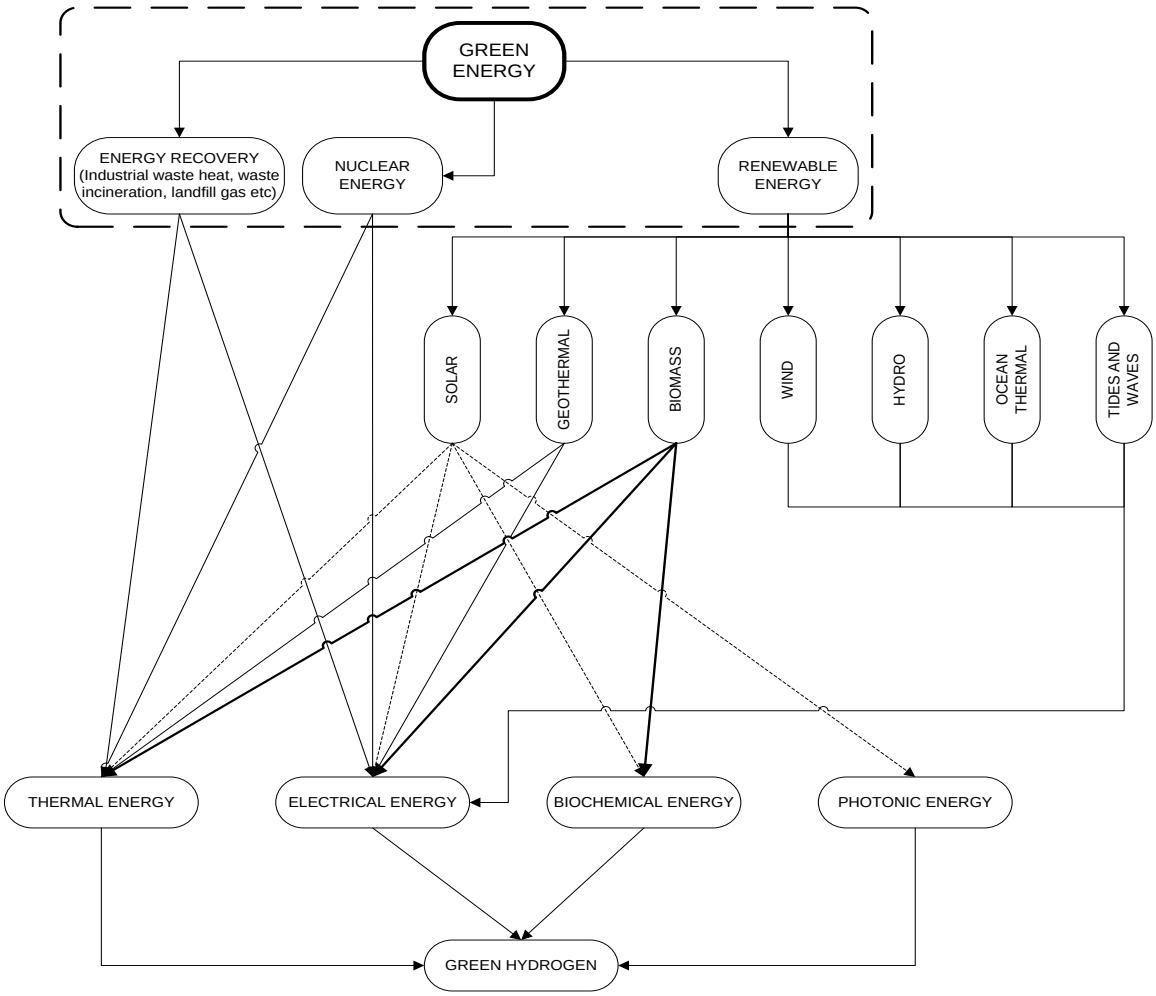

Figure 1.3: Paths of generation of basic form of energy from primary green energy sources (Adapted from [16])

Although large amount of hydrogen is currently produced from fossil fuels, this causes the emissions of large quantities of CO_2 into the atmosphere. Thus, the production of hydrogen from renewable sources will be more important in the future. Figure 1.3 shows green energy sources to produce hydrogen with zero – emissions into the atmosphere. Cost, difficulties of large amount of hydrogen production, and low efficiency are important issues regarding hydrogen

production from renewable energy sources, so it seems that fossil fuels are used to satisfy global hydrogen demand in short and intermediate terms.

There are many methods such as steam methane reforming, partial oxidation, autothermal reforming, thermochemical water splitting, and water electrolysis for hydrogen production by using different energy sources. Table 1.1 summarizes energy sources, energy needs and emissions in the different hydrogen production processes.

Table 1.1: Sources, energy needs and emissions in the different hydrogen production processes (Adapted from [17])

Methods		Processes	Hydrogen sources	Energy and/or Chemical requirements	By products emissions
Thermal	T1	Steam reformation	Natural gas Biogas	High temperature (HT) and high pressure (HP)	CO_2, CO
	T2	Partial oxidation	Hydrocarbons	HT and HP	CO_2, CO, CH_4, C
	T3	Thermochemical Water splitting	Water	HT from nuclear reactors and chemicals (H_2SO_4, ZnO, I_2...)	
	T4a	Thermolysis/ Gasification	Coal	HT and HP	CO_2, CO, CH_4, C
	T4b	Thermolysis/ Gasification	Biomass	HT and HP	CO_2, CO, CH_4, C
Electro-chemical	E1	Electrolysis	Water	Electricity	
	E2	High temperature electrolysis	Water	Electricity and HT from nuclear reactor	
	E3	Photolysis	Water	Solar	
Biological	B1	Photobiological	Water	Algae and solar	
	B2	Bacterial fermentation	Biomass	HT	CO_2, CO, CH_4

Steam reforming is currently the least expensive and most commonly used method for hydrogen production. This process is an endothermic, catalytic process and natural gas is

generally used as feed. The main advantages of steam methane reformation (SMR) are given as follows [18]:

- It is the most economical method for hydrogen production.
- This process does not need oxygen.
- SMR has the lowest process temperature.
- It is the best H_2/CO ratio for H_2 production.

On the other hand, the main disadvantage of the SMR is that this process has highest air emissions [18, 19]. SMR basic chemical reactions can be described by the following equations [20]:

$$C_nH_m + nH_2O \rightarrow nCO + \left(n + \frac{m}{2}\right)H_2 \quad \Delta H < 0 \tag{1.1}$$

$$CH_4 + H_2O \leftrightarrow CO + 3H_2 \qquad \Delta H = -206\,\frac{kJ}{mol}\ \text{at}\ 15℃ \tag{1.2}$$

$$CO + H_2O \leftrightarrow CO + H_2 \qquad \Delta H = +41.2\,\frac{kJ}{mol}\ \text{at}\ 15℃ \tag{1.3}$$

Partial oxidation (POX) is the second most common method for hydrogen production. POX does not need a catalyst. The temperature range for non-catalytic POX is between 1150 and 1315 ℃ [20]. Disadvantages of POX are very high processing temperatures, low H_2/CO ratio, and process complexity [18]. Basic chemical reaction of POX is shown as follow and this reaction is considered as a faster reaction than steam reforming [18, 20]:

$$C_mH_n + \frac{1}{2}mO_2 \rightarrow mCO + \frac{n}{2}H_2 \quad \Delta H > 0 \tag{1.4}$$

Coal gasification process is another method for hydrogen production and it is competitive with SMR if oil and/or natural gas are expensive. Firstly, partial oxidation of coal occurs in a gasifier at high pressure and high temperature. After this reaction, syngas that consists of mainly

CO, CO_2, H_2, and H_2O is obtained. High and low temperature shift reactors are used to increase amount of hydrogen in the syngas. Then, CO_2 and H_2S are removed in acid gas removal unit. Finally, H_2 is obtained by using pressure swing adsorption (PSA). Remaining gas, which is tail gas, is used to produce power. Simply flow diagram of hydrogen production from coal gasification is shown in Figure 1.4. Some reactions of gasification of coal are given as follows [21]:

$$C + H_2O = CO + H_2 \quad (1.5)$$

$$C + O_2 = CO_2 \quad (1.6)$$

$$C + 0.5O_2 = CO \quad (1.7)$$

$$C + CO_2 = 2CO \quad (1.8)$$

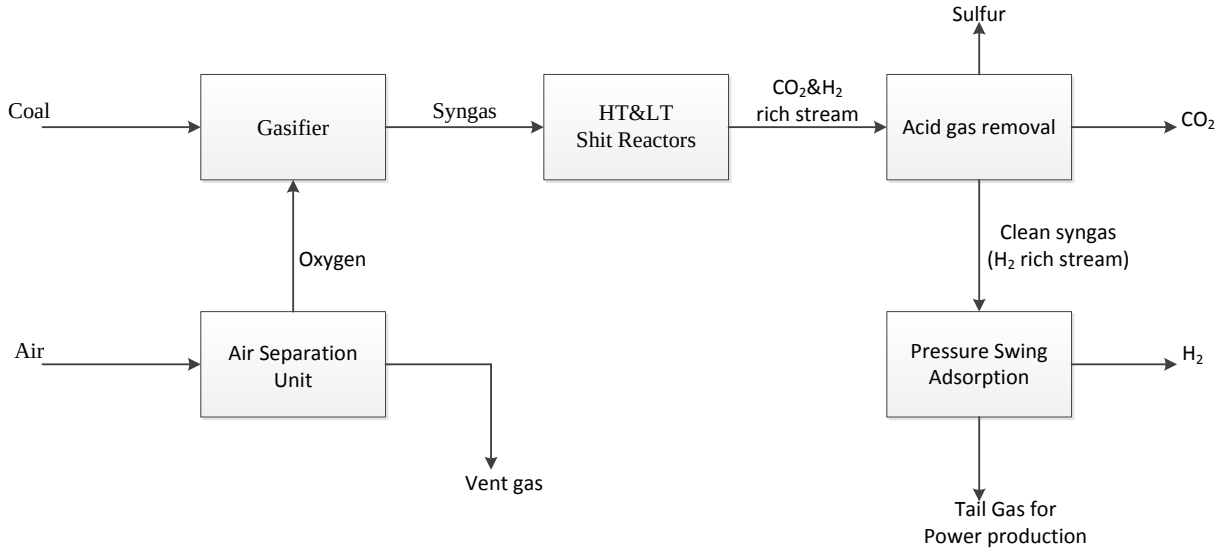

Figure 1.4: Simple flow diagram of hydrogen production from coal gasification

Hydrogen can also be directly produced from water using water electrolysis. The water molecule is separated hydrogen at the cathode and oxygen at the anode in electrolysis process in which a direct electric current passing two electrodes through an ionic substance. An electrolyzer is called a device that performs electrolysis. It can also be defined as a device that can convert electrical energy into chemical energy [22]. The proton exchange membrane (PEM) and alkaline process are commonly used for water electrolysis. There are two important parameters: the efficiency and the current density for these processes. The current density for PEM electrolyzer is higher than 1.6 Acm^{-2} and its efficiency is in the range of 50 and 75 % based on the lower heating value of hydrogen [16, 18]. In the PEM electrolyzer the following reactions take place at anode and cathode [22]:

Anode: $H_2O\ (liq) \rightarrow 1/2O_2\ (g) + 2H^+ + 2e^-$ (1.9)

Cathode: $2H^+ + 2e^- \rightarrow H_2\ (g)$ (1.10)

Overall: $H_2O\ (liq) \rightarrow H_2\ (g) + 1/2O_2\ (g) \quad \Delta H=-288\ kJmol^{-1}$ (1.11)

Although PEM electrolysis process has high efficiency, the main disadvantage of it is that this is an expensive technology [22]. The typical efficiency of alkaline electrolyzer is 50 – 65%, and the current density is 0.1 – 0.4 Acm^{-2} [16]. Only inexpensive materials are used for alkaline electrolyzer; however, challenges regarding this technology are concerning the lifetime of systems and maintenance costs [22]. The overall reactions in the alkaline electrolyzer take place at the anode and cathode [18]:

Anode: $4OH^- \rightarrow O_2 + 2H_2O$ (1.12)

Cathode: $2H_2O + 2e^- \rightarrow H_2 + 2OH^-$ (1.13)

Overall: $H_2O\ (liq) \rightarrow H_2\ (g) + 1/2O_2\ (g) \quad \Delta H=-288\ kJmol^{-1}$ (1.14)

PEM and alkaline electrolysis processes consume high amount of electrical energy. Hydrogen can be produced using high temperature electrolysis with lower electrical energy consumption. Part of the electrical energy replaces with thermal energy to split water in this process. This technology has very high efficiency. It has been reported that high temperature water electrolysis efficiencies are close to 100% at the laboratory scale at high current densities [22]. Other advantages of this technology are that an electrocatalyst is not required for high temperature water electrolysis, so this decreases the cost, and large amounts of hydrogen can be produced using the high temperature heat released by nuclear reactor [22].

Thermochemical water splitting processes can also be used to produce hydrogen from water. In these processes, heat is used as a primary energy source rather than electricity for splitting water to produce hydrogen. High temperature heat in the range of 500 – 1200 ℃ is necessary for the chemical reactions in the thermochemical water splitting processes [18]. Although there are about two hundred thermochemical cycles that have been reported to produce hydrogen, sulfur – iodine (S-I) and copper – chlorine are two important cycles among these cycles [23].

There are several types of S – I cycles; however, three –step cycle is the most common cycle for thermal decomposition of water [18, 23]. The first step is called the Bunsen reaction that is hydrolysis step, the second step is the decomposition of sulfuric acid. Oxygen is produced in this step. The third step is the acid HI decomposition step; hydrogen is obtained in this step. The chemical reactions of S-I cycle are given as follows [23]:

Step 1: Hydrolysis step (exothermic)

$$I_2\ (l+g) + SO_2\ (g) + 2H_2O\ (g) \rightarrow 2HI\ (g) + H_2SO_4\ (l),\ \text{at } 393\ K \qquad (1.15)$$

Step 2: Oxygen production step (endothermic)

H_2SO_4 (g) → SO_2 (g) + H_2O (g) + 0.5O_2 (g), at 1123 K (1.16)

Step 3: Hydrogen production step (endothermic)

2HI (g) → I_2 (g) + H_2 (g), at 723 K (1.17)

Several types of step cycles can also be used for Cu-Cl cycle. However, two-, three-, and four-step cycles have lower efficiency and more engineering challenges than the five-step Cu-Cl cycle [23]. There are five main chemical reactions that take place in the five-step Cu-Cl cycle are given as follow [23]:

Step 1: Chlorination step (exothermic)

2Cu (s) + 2HCl (g) = 2CuCl (molten) + H_2 (g), at 723 K (1.18)

Step 2: Disproportionation step (electrolysis)

4CuCl (aq) = 2Cu (s) + 2$CuCl_2$ (aq), in aqueous solution of HCl, at 303-353 K (1.19)

Step 3: Drying step (endothermic)

$CuCl_2$ (aq) + $n_f H_2O$ (l) = $CuCl_2.n_h H_2O$ (s) + (n_f-n_h) H2O (1.20)

where n_f and n_h are mole of free water, and mole of hydrated water, respectively, and n_f>7.5, n_h is 0-4, at 303-353 K (crystallization) or 373-533 K (spray drying).

Step 4: Hydrolysis step (endothermic)

$2CuCl_2.n_h H_2O$ (s) +H_2O(g) = $CuOCuCl_2$ (s) +2HCl (g) +$n_h H_2O$ (g), n_h is 0-4, at 648 K (1.21)

Step 5: Decomposition step (endothermic)

$CuOCuCl_2$ (s) = 2CuCl (molten) + 0.5O_2 (g), at 773-803 K (1.22)

Global hydrogen production is around 40.5 million tonnes [24], and is estimated that hydrogen demand will grow over 4% yearly through 2016 [25]. The most of produced hydrogen

using different methods is currently used for ammonia production, which is 54% of the global hydrogen demand, and chemical industry/oil refinery, which is about 35% of global hydrogen demand [20]

1.3 Literature Review

Coal gasification system is becoming more appealing day by day because of increasing oil prices and the large amount of coal reservoirs. In addition, coal gasification system is relatively more environmentally friendly if it is used with carbon capture and storage technology; in addition, liquid fuels can be produced using coal gasification systems. Therefore, many studies have been currently undertaken on various aspects of coal gasification systems. These studies can be classified as electricity production from coal gasification using IGCC power plants, liquid fuel and production of other chemicals from coal gasification, and co – production of electricity and hydrogen from coal.

Bhattacharya *et al.* [26] used steady – state simulation tool to optimize thermal efficiency of an integrated gasification combined cycle plant with CO_2 capture. In this study, global design decisions such as the amount of CO_2 capture in the Selexol unit, the optimal carbon monoxide conversion in the water – gas shift reactors; local design decisions in different subsections such as the Selexol and the Claus unit; and operating conditions were considered to optimize the system. The net plant efficiency obtained was 5% higher than a previously published data.

Heat transfer fluids such as liquid metal, molten salt were used to improve heat recovery in the General Electric (GE) gasifier by Botros and Brisson [27]. Hot syngas in the gasifier must be cooled before the acid gas removal process. In the GE gasification process, syngas heat is absorbed by steam, but it is not possible to produce superheated steam at high pressures in the

radiant heat exchanger in the gasifier due to maximum allowable hoop stress. Botros and Brisson produced superheated steam at high pressures in the radiant heat exchanger using intermediate heat transfer fluids, thus IGCC plant efficiency changes by about 0.7%-points.

Botero *et al.* [28] used liquid carbon dioxide as a slurrying medium instead of water – slurry to improve the efficiency of low rank coal gasification in integrated gasification combined cycle power plants with carbon capture. The advantages of slurry – fed for entrained – flow gasifiers are that slurry – fed is more simple and cheaper than dry – fed method, and high pressures can be achieved; however, water in the coal slurry causes low gasifier efficiency because of high enthalpy of vaporization of water. Botero *et al.* suggested liquid carbon monoxide as a slurry medium because its enthalpy of vaporization is lower than water. The results show that a power generation efficiency improvement is about up to 25%.

Adams and Barton [29] suggested a novel process to produce electricity with zero emissions and high efficiency. They integrated solid oxide fuel cell (SOFC) and the gasification process to increase the system efficiency. The efficiency of the SOFC-based system with cooling towers was found to be ~44.8%, while the efficiency of the integrated gasification combined cycle systems was about 38.2%. Moreover, they achieved capturing and sequestering almost 100% of CO_2 and other pollutants (e.g. SO_x, NO_x).

Siefert and Lister [30] compared two different gasification systems. The first system is an integrated gasification combined cycle with advanced H_2-O_2 membrane separation including CO_2 sequestration (IGCC-CCS). The second system is an integrated gasification fuel cell cycle with a catalytic gasifier as well as a pressurized SOFC including CO_2 sequestration (IGFC-CCS). They accomplished the exergy and economic analyses of these systems.

The novel membrane and syngas chemical looping processes for production of coal-based hydrogen and electricity were examined by Li *et al.* [31]. They found that the novel membrane and syngas chemical looping strategies are promising methods to reduce the energy and cost penalties for CO_2 capture from coal conversion systems.

Ghosh and De [32] performed an exergy analysis of a cogeneration plant using coal gasification and SOFC. They found the exergy destruction of different components of the system. Their results show that the highest exergy destruction takes place in the gasifier and SOFC.

A polygeneration system was evaluated to produce electricity, naphtha, diesel and methanol from coal and biomass by Chen *et al.* [33]. In this study, the optimal design and operation of polygeneration systems were investigated under different price scenarios.

To produce different chemical products using coal gasification system, H_2/CO ratio must be a certain amount. For example H_2/CO ratio must be in the syngas about 1.0 to produce dimethyl ether (DME), and about 2.0 for direct methanol synthesis and the Fisher – Tropsch (FT) processes. Although H_2/CO ratio is enough to produce DME from the gasification of coal or biomass, it is not enough for direct methanol synthesis and FT processes. A novel process was proposed for efficient polygeneration from coal gasification by Adams and Barton [34]. They used coal gasification and natural gas reforming to obtain a H_2/CO ratio of 2.

Chiesa *et al.* [35, 36] investigated the economic and technical performance of coal gasification system to produce H_2 and electricity, with CO_2 capturing and storage. They used different methods of syngas heat recovery and evaluated effects of the electricity/H_2 ratio, gasifier pressure, and hydrogen purity on the system performance.

Xu *et al.* [37] proposed coal partial gasification with CO_2 capture system for co-production of hydrogen and electricity. They could attain the system overall exergy efficiency of ~54.3%, and the ratio of hydrogen to electricity (kW H_2/kW electricity) of ~4.76.

Liszka *et al.* [38] analyzed hydrogen-oriented coal gasification system for two different cases, namely coal only, coal and biomass operation systems. In addition, they evaluated exergy losses for in the main components of the system. The highest exergy loss was calculated for the gasifier.

Cosmos *et al.* [39] investigated technical performance of hydrogen production based on coal gasification with carbon dioxide capturing technology. To increase syngas pressure, they proposed the use of a syngas compressor for the dry feed gasifier after the gas quench and before the shift conversion.

1.4 Objectives and Outline of the Thesis

Although there are many studies in the open literature, these studies generally focus on co-production using coal gasification system, and one type of coal is commonly used to feed the gasifier. In addition, many works do not include exergy analysis in detail and effects of different parameters on the hydrogen production in the system. In the present study, a novel integrated hydrogen production system which combines coal gasification and alkaline water electrolyzer systems is thermodynamically modeled, and its performance is evaluated through exergy efficiency. The power required for this system is completely generated in the system; thus no need to connection to electric grid. The carbon dioxide produced is also captured in this system; thus this system is an environmentally friendly system.

Main objectives of this study are given as follows:

- To develop a novel integrated system to produce hydrogen from coal gasification and alkaline water electrolyzer.
- To analyze the system thermodynamically using energy and exergy methodologies.
- To study performance of the system through energy and exergy efficiencies.
- To conduct parametric studies to investigate the effects of water ratio in coal slurry, gasifier temperature, hydrogen recovery efficiency of the pressure swing adsorption unit and carbon dioxide removal ratio on the hydrogen production.
- To study effects of different types of coals on power consumption, power production, emission performance and hydrogen production in the system.

This thesis is organized in six chapters. Global energy demand, use of energy sources, and predictions about future energy demand in the world, hydrogen production methods, and current studies about coal gasification are given in Chapter 1. System components in the system that is studied in this thesis are explained in Chapter 2. Simulation of the system using Aspen Plus is mentioned in Chapter 3. In addition, some background information about Aspen Plus is mentioned in Chapter 3. Chapter 4 provides information about thermodynamic modeling of the system. Chapter 5 includes results of energy and exergy analyses, parametric studies, and effects of different types of coals on the system. Conclusions and recommendations for future studies are given in Chapter 6.

Chapter 2

System and Process Description

2.1 Overview

In this thesis, a combined coal gasification and alkaline water electrolyzer system for hydrogen production is investigated. The studied system is shown in Figure 2.1. The main components of this system are a GE coal gasifier, an air separation unit (ASU), a high and a low temperature water gas shift (WGS) reactors, H_2S and CO_2 removal units, a pressure swing adsorption (PSA) unit, a combustor, an alkaline water electrolyzer, a heat recovery steam generator (HRSG), and a power generation unit. Firstly, syngas is produced using the gasifier; water gas shift reactors are used to convert CO to CO_2 and increase the amount of hydrogen in the syngas; then H_2S and CO_2 are removed in the acid gas removal unit; after the acid gas removal process, hydrogen is recovered by using the PSA. Remaining tail gas from the PSA unit is evaluated in the combustor to produce hot flue gas. Heat is recovered from the hot flue gas in the HRSG to produce steam. In addition, heat is recovered in different parts of the system to produce steam. Steam is used to produce power and for some processes such as for high temperature water gas shift reactors in the system. Power requirements for power consumer components in the system calculated, and the power is provided for these components from produced power. Remaining produced power is used in the alkaline water electrolyzer to produce extra hydrogen.

Main system components and process are described as follow parts in the chapter.

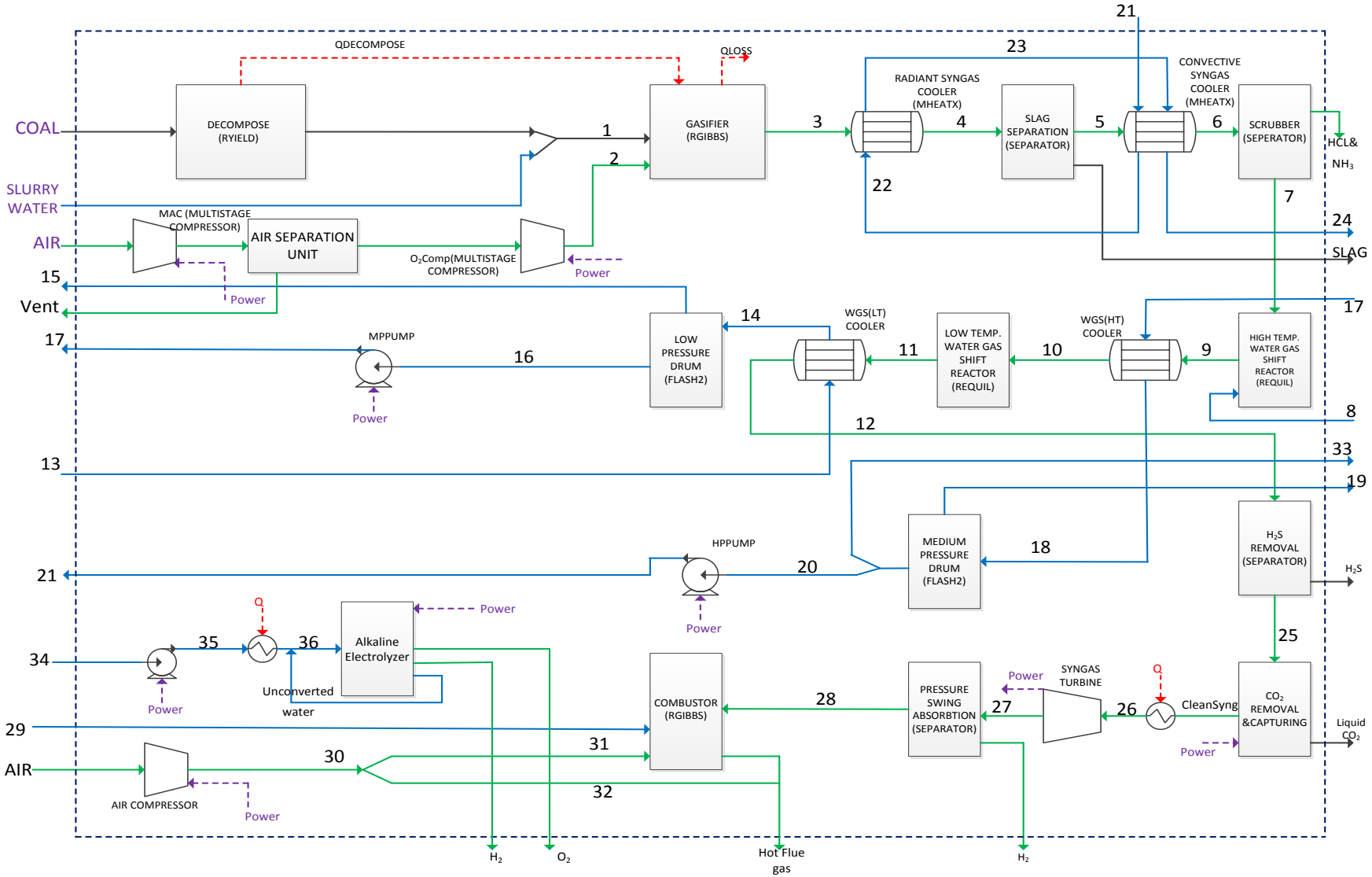

(a) The main system

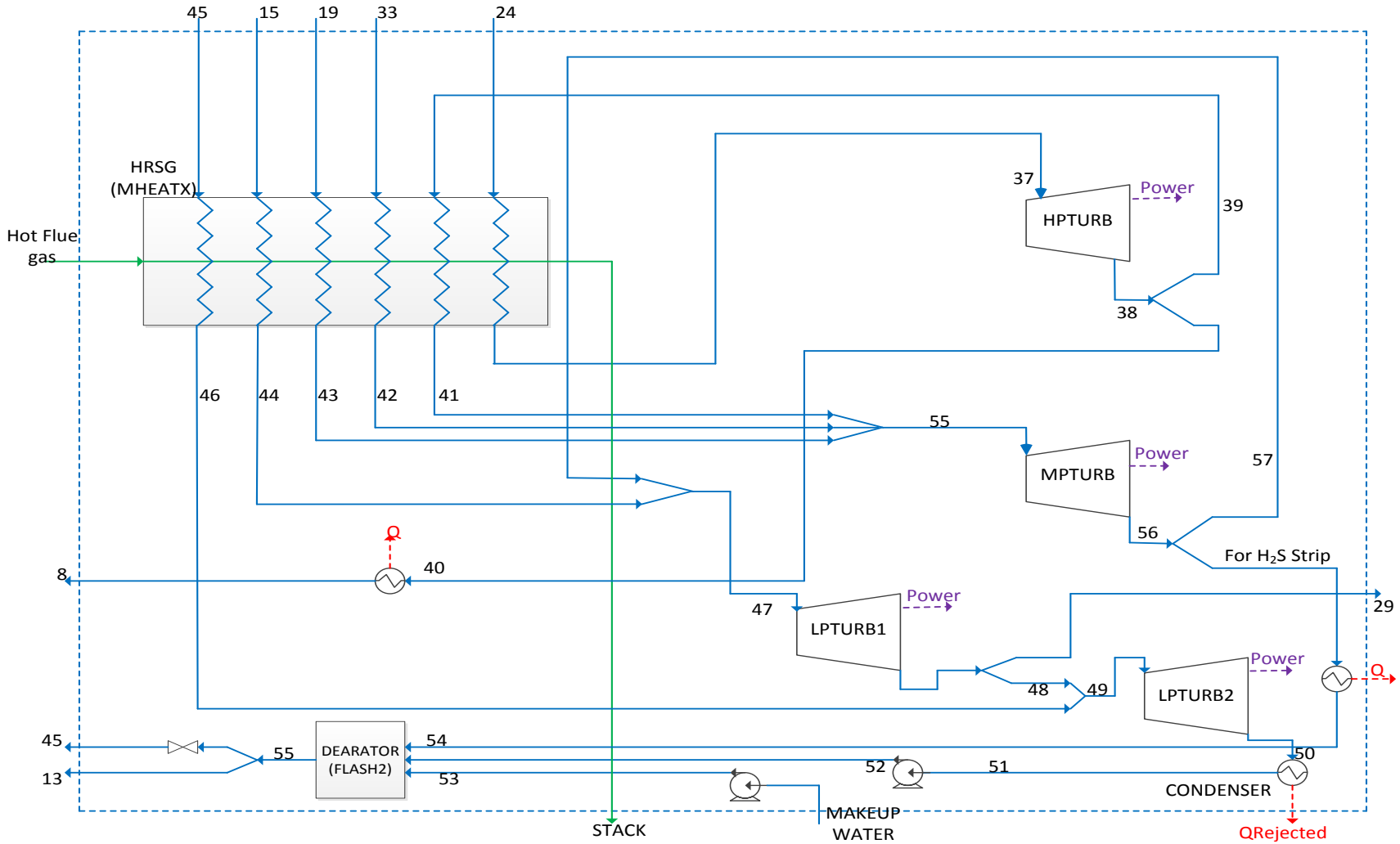

(b) The steam cycle unit of the system

Figure 2.1: The combined coal gasification and alkaline water electrolysis system, (a) the main system, (b) the steam cycle unit of the system.

2.2 Gasifier

The most important component of a coal gasification system is the gasifier where coal gasification takes place. The difference between combustion and gasification of the coal is that the gasification takes place in oxygen – lean environment. Thus, syngas that consists of CO, H_2, H_2O, CO_2 and small amount of other impurities such as NH_3, H_2S is obtained in the gasifier. Three types of gasifiers that are moving – bed gasifiers, fluid – bed gasifiers, and entrained – flow gasifiers can be used for gasification process. However, entrained – flow processes are commonly used in the market because of the largest treatment ability and the smallest environmental impact of the entrained – flow process [21]. Shell and GE coal gasifiers are two well – known entrained – flow type gasifier technology.

Shell coal gasifier is a dry – feeding entrained – flow gasifier. It operates with oxygen at temperatures ranging from 1500℃ to 1600℃, and pressures ranging from ~2.4 MPa to ~4.5 MPa [40]. Quenching with cooled recycle product gas is used to decrease the temperature of the syngas, and the further cooling in the waste heat recovery unit, which consists of radiant, superheating, convection, and economizing sections, where high – pressure superheated steam is generated. This process is illustrated in Figure 2.2. Shell coal gasifier has high cold gas efficiency is about 82% and the carbon conversion is over 99% [21], thus IGCC power plants has higher thermal efficiency. However, complexity of dry – feeding system, the low gasification pressure, and the high capital cost are the main disadvantages of the Shell coal gasifiers.

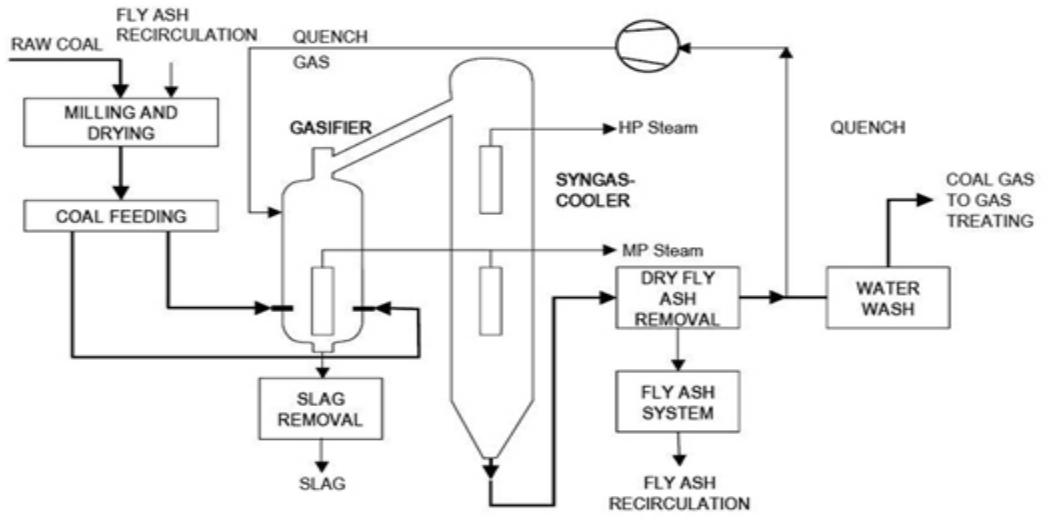

Figure 2.2: A simplified Shell coal gasifier scheme (From NETL website [41])

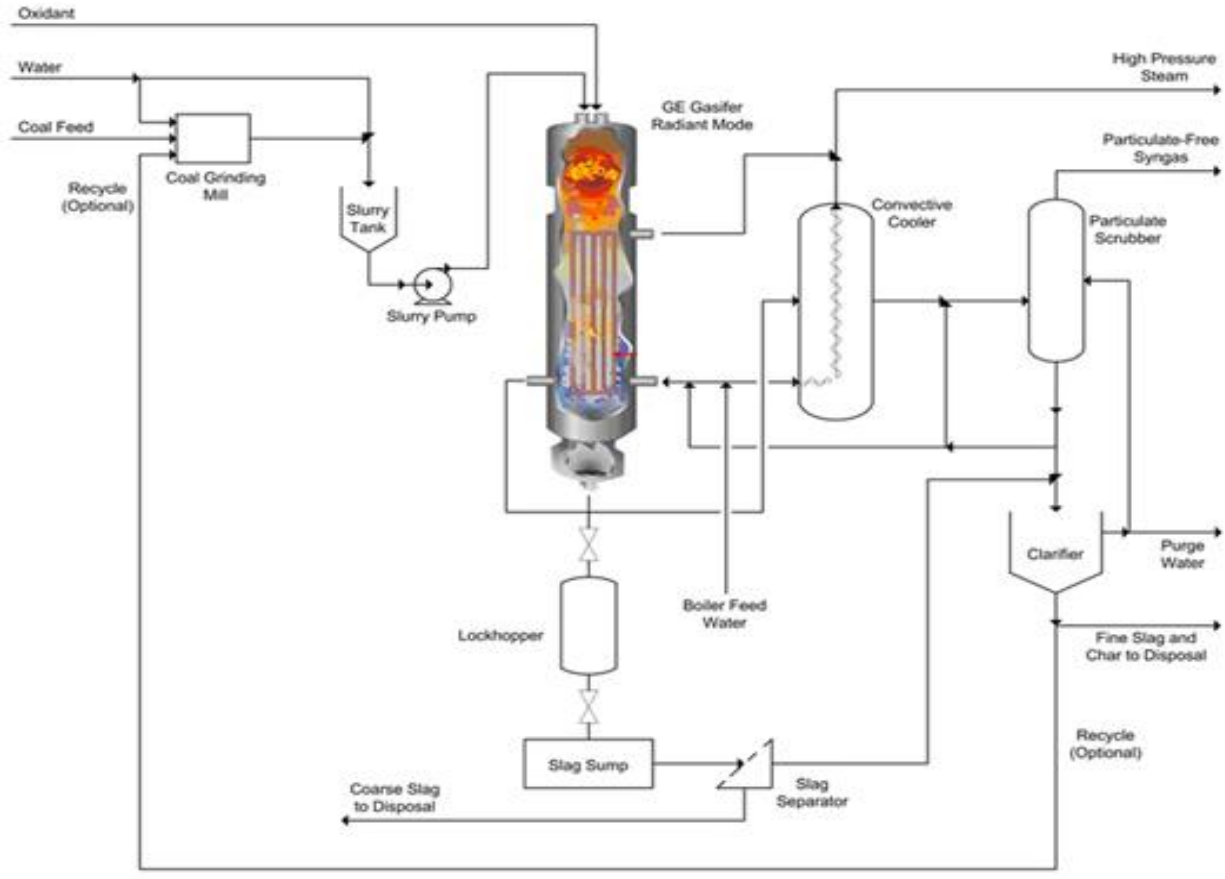

Figure 2.3: GE coal gasifier with Radiant and Convective coolers (From NETL website [42])

In this study, GE entrained – flow gasifier with radiant and convective cooling is selected as the gasifier of the system. Coal/water slurry with a ratio of 60%-70% and oxygen with a purity of 95%, provided by the ASU, and are fed to this gasifier to produce syngas [40]. The GEE gasifier can operate at pressures in excess of 62 bars and a temperature in the range of 1230°C to 1595°C [43, 44]. Operation at high pressures is beneficial for the gasifier because it decreases the gasifier volume, and as a result, reduces the capital cost [43]. In addition, high operation pressures of the gasifier are beneficial for chemical production processes, such as the operating pressures ranges from 8.5 MPa to 10 MPa in the ammonia industry, and the 6-7 MPa in methanol industry [21]. Another advantage of GE coal gasifier is that its capital cost is lower than dry –feeding systems. It has been estimated that the coal preparation and feed system of the dry – feeding gasifiers are three times more expensive than the equipment of slurry – fed gasifier for equal electrical output [28]. Typical syngas composition for a slurry feed gasifier consists of CO (35%-45%), CO_2 (10%-15%), H_2 (27%-30%), H_2O (15%-25%), H_2S and COS (0.2%-1%) [45]. Quench, radiant or combination of radiant and convective cooling methods can be used to decrease the temperature of hot syngas and heat recovery. Heat exchangers are used for the radiant and convective cooling, while water is sprayed onto the hot syngas in the quench design. The quench design is more reliable and cheaper than other radiant and convective designs [35]; however, it has lower thermal efficiency, because high pressure steam cannot be produced through this method [35]. In addition, large quantities of water are used in a water quench system; thereby causes additional issues such as the need for larger water treatment facilities, increased discharge water permitting problems, and added operating and maintenance costs compared to the radiant and convective design [43]. High pressure steam is produced during cooling operation using radiant and

convective coolers that is shown in Figure 2.3. To this end, after the syngas cooling operation, a scrubber is used to remove HCl and NH_3 from the syngas. Then, particulate free syngas feeds to the WGS reactors for CO and COS conversion.

2.3 Air Separation Unit

The gasifier size may be reduced, smaller gas handling and equipment and heat exchangers can be employed, and higher syngas heating value can be obtained if oxygen is used instead of air in the gasification process [43]. In addition, the partial pressure of CO_2 is higher in oxygen blown gasifier syngas, so this decreases cost and increases effectiveness of the CO_2 removal unit [44]. For such reasons, an ASU is used in this system to produce oxygen. Once oxygen is produced in the ASU, and its pressure increases to 1.2 times the gasifier pressure in a multistage-compressor [35]. The pressurized oxygen is utilized during partial oxidation of the coal slurry in the gasifier. It is noted that the ASU consumes high amount of power. Of course, this power can be minimized by optimization of the oxygen product volume, purity and pressure, which is beyond the scope of this thesis.

Nitrogen and oxygen are separated from atmospheric air using a cryogenic ASU. Firstly, ambient air enters the multistage compressor, then molecular sieve adsorbs is used to remove residual water vapor, carbon dioxide, and atmospheric contaminants, which is shown in Figure 2.4. After the cooling process of the compressed air, N_2 and O_2 are separated using low pressure and high pressure columns. The basic principle behind the separation of nitrogen and oxygen in an ASU is that the vapor pressure of nitrogen is always higher than that of oxygen, so oxygen has a less volatility than nitrogen [47].

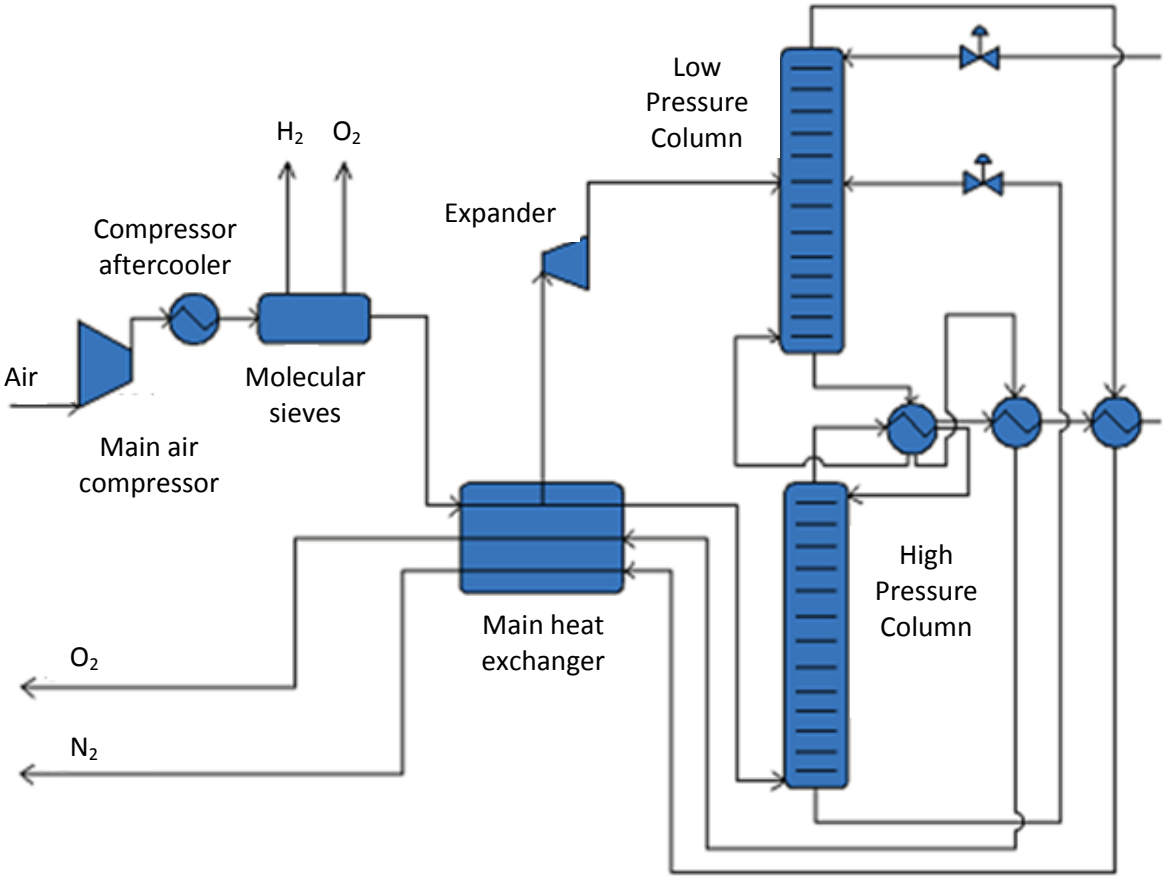

Figure 2.4: Simple flow diagram of an ASU (Adapted from [46])

2.4 Water Gas Shift Reactors

High- and low – temperature WGS reactors in series with a cooler are used in this study to convert CO to CO_2 through Reaction (1) to produce more hydrogen. The conversion of COS to H_2S through Reaction (2) is also taken place in the WGS reactors:

$CO + H_2O \rightarrow CO_2 + H_2$ ΔH_{rxn}= -41.1 kJ/mol (2.1)

$COS + H_2O \rightarrow CO_2 + H_2S$ ΔH_{rxn}= -33.7 kJ/mol (2.2)

The aim of using the WGS reactors is not only to obtain more hydrogen but also production of hydrogen with minimal negative impact on the environment. Since the solubility of CO_2 in the Selexol solvent is about 19 times greater than it is for CO, and for H_2S is approximately 4 times greater than it is for COS [48], CO_2 and H_2S can be removed easily in the Selexol solvent. Therefore, SO_x and CO_2 emissions from the system decrease.

The equilibrium constant of the water gas shift reaction (Eq.2.1) can be calculated from the below equation [49]:

$$\ln (K_{eq}) = -2.4198+0.0003855T+2180.6/T \quad (2.3)$$

As shown in Figure 2.5, the equilibrium constant that is calculated using Eq.2.3 is higher for low temperatures, so low temperatures are favorable for water gas shift reaction; however, high temperatures are more favorable for the kinetics of the catalytic reaction [49]. Therefore, high and low temperatures WGS reactors are used with together in the system.

The WGS reactors operate in a range of temperatures. At low and high temperatures, WGS reactors operate at 150℃ - 300℃ and 350℃ - 600℃, respectively [49]. The operating pressures of the WGS reactors that depend on plant requirements range above 20 bars and sometimes higher than 30 bar [21]. Different catalysts such as copper – based, iron – based, nickel – based, gold – based catalysts are used in the two different stages [49]. Iron – based and copper – based catalysts can be used for the high and low temperature WGS reactors for the studied system, respectively. Because H_2S is removed after the WGS reactors, the catalysts must be sulfur tolerant.

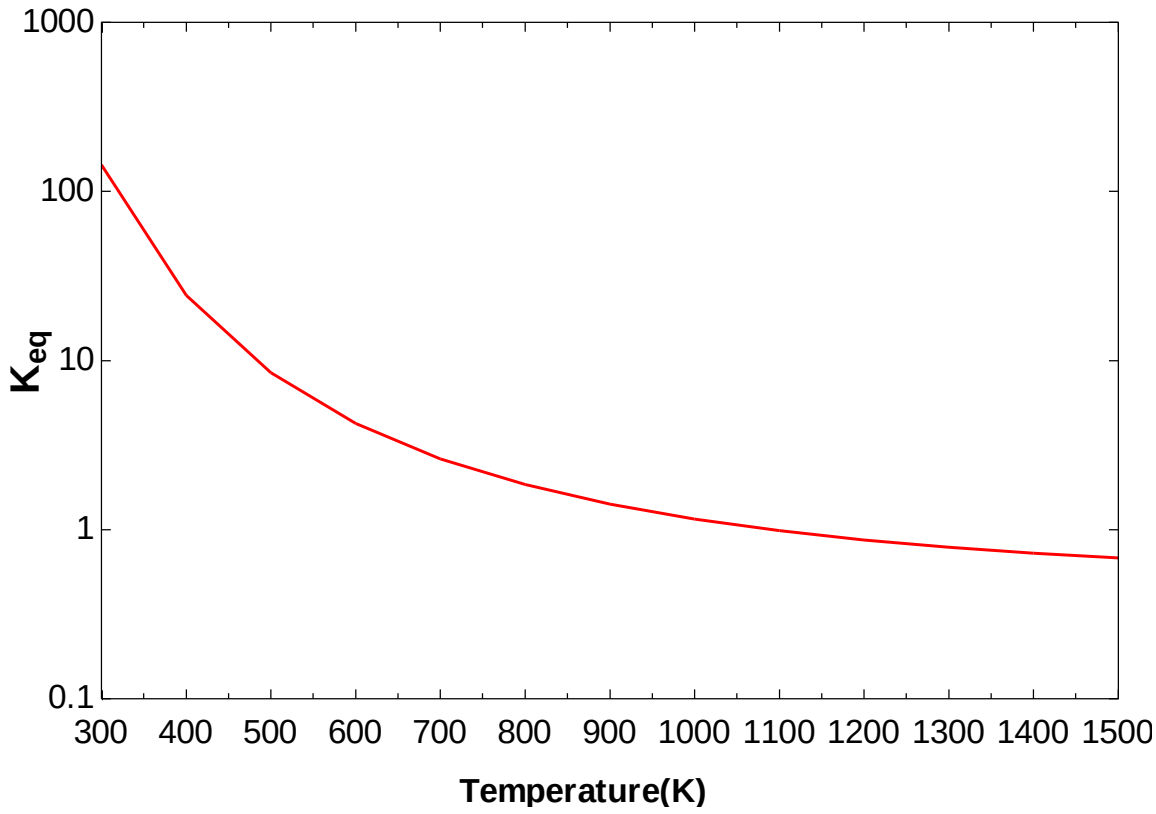

Figure 2.5: Variation of the equilibrium constant of the water gas shift reaction with change of temperature

2.5 Acid Gas Removal Unit

There are three different methods to remove acid gases from syngas. These methods are included in the chemical absorption, physical absorption, and physical and chemical absorption [50]. These chemical reactions occur between acid gas components and solvent molecules and dissolve into the solvent in the chemical absorption process, while the components are physically absorbed into the solvent molecule in the physical absorption process [50].

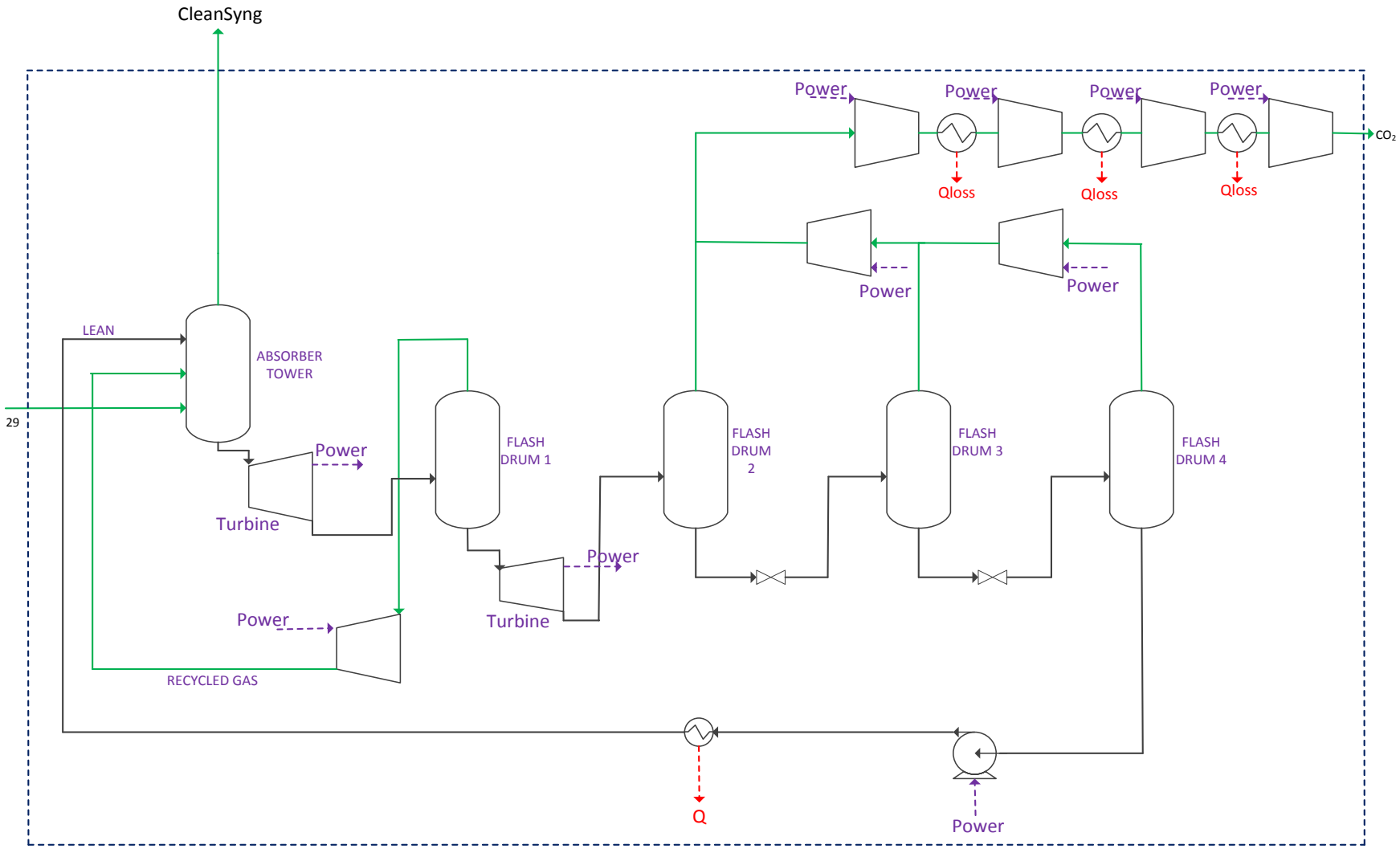

Figure 2.6: Flow diagram of CO_2 removal and capturing (Based on [51, 52])

Rectisol and Selexol are two important physical solvent that are commonly used to remove H_2S and CO_2 from syngas. Selexol (di – methyl – ethers of polyethylene glycol) is preferred as a solvent for the system in the thesis because it is appropriate for high pressure applications with moderate cost [21].

In this study, two – stage Selexol acid/gas removal unit is used to remove H_2S and CO_2. First, H_2S is removed and then. CO_2 is removed using the physical solvent Selexol. Since power consumption of the H_2S removal is not an important contribution on the total power consumption of the system, it is not analyzed in detail. However, CO_2 removal part is an important power consumer. Therefore, the system that is shown in Figure 2.6 is used to estimate power consumption of CO_2 removal. It is mentioned in more detail in Chapter 3. After the acid gas removal unit, the clean syngas feeds to the PSA unit to recover hydrogen.

2.6 Pressure Swing Adsorption

The PSA unit is used to recover hydrogen from clean syngas. The optimum pressure of the PSA unit is in the range of 15 – 30 bars [53], the temperature range from 21℃ to 38℃ [21], and the hydrogen recovery efficiency of this unit lies in the range of 70 – 90% [54]. Hydrogen that is produced from the PSA can be used in PEM fuel cell, because high purity hydrogen can be produced using the PSA. Typical purities range of recovered hydrogen is from 99 to 99.999 mol% [53].

The basic principle of the PSA is that adsorbent of the impurities while hydrogen is not adsorbed. The basic flow schema of a PSA unit is shown in Figure 2.7 [54]. Multiple adsorbers are used in a PSA unit to provide constant feed, product, and offgas flows. Recovered hydrogen from the PSA unit is obtained about same pressure of the feed gas, and the offgas (tail gas) is at

low pressure [54]. In the present study, hydrogen is recovered at 35℃ and 2 MPa and the PSA unit hydrogen recovery efficiency is assumed to be 85% [35] for base case simulation. Tail gas is used in the combustor to produce hot flue gas.

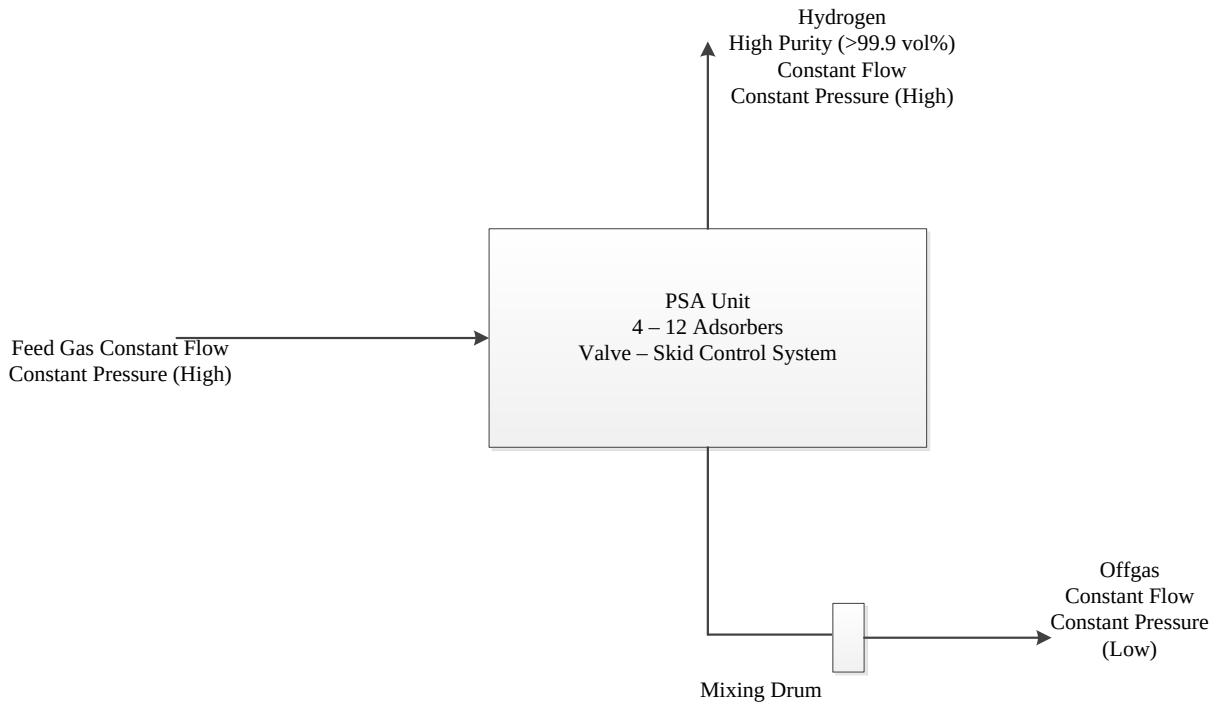

Figure 2.7: PSA basic flow schema (Adapted from [54])

2.7 Heat Integration and Power Production

Heat is recovered from the radiant and convective coolers, the WGS reactors coolers, and hot flue gas in the system, and is used for power generation. Low quality heat such as heat from multistage compressors is not used for power generation. Hot flue gas is produced using purge gas from the PSA unit in the combustor. To decrease NO_x formation, steam is injected into the combustor. Saturated vapor at 13 MPa is produced using heat from the radiant cooler. The convective cooler heat is used to produce saturated liquid and superheated steam at 13 MPa. Medium and low pressure steam is produced using the WGS reactors coolers. Hot flue gas is used to produce superheated steam at 565℃ and 13 MPa, reheating, and superheated steam at 4 MPa, 0.4 MPa, and 0.15 MPa.

A steam cycle is used for power generation instead of a gas turbine combined cycle to decrease the system capital cost; however, a detailed cost analysis is required to make the final decision. Power is also produced using syngas turbine before the PSA unit.

2.8 Alkaline Electrolyzer

To increase the hydrogen production, an alkaline water electrolyzer is employed in this system. Although high purity of hydrogen can be obtained using water electrolysers, it is not commonly used due to its relatively high cost. The main reason for its high cost is the high amount of electric power required for water electrolysis [55, 56]. Some commercial electrolysis systems and the main characteristics of them are shown in Table 2.1.

Table 2.1: Conventional electrolysis systems (Adapted from [57])

Manufacturer companies	Lurgi system	MTU	Teledyne	Hydrogenics	Norsk Hydro	ABB & Cie
Cell type	bipolar	bipolar	bipolar	bipolar	bipolar	bipolar
Operating pressure (bar)	30	30	7	10/25*	Atmospheric	Atmospheric
Operating temperature (℃)	90	130	80	-	80	80
Electrolyte	25%KOH	30%KOH	KOH	30%KOH	25%KOH	25%KOH
Current density (A/m^2)	2000	7000-10000	3000	-	-	2000
Cell voltage (V)	1.86	1.65-1.8	-	-	-	2.04
Current efficiency (%)	98.75	>99.5	-	-	99.9	99.9
Power cons. (kWh/Nm^3)	4.3-4.65	4-4.4	5.6	4.2	4.3	4.9
Maximum prod. rate (Nm^3/h)	760	-	140	60	100	-

In this study, all power requirements of the system components are generated in the steam cycle unit inside the system. Indeed, the remaining power is utilized to produce extra hydrogen in the alkaline water electrolyzer.

Chapter 3

System Simulation

3.1 Overview

The simulation of the combined coal gasification and alkaline water electrolyzer system was carried out by Aspen Plus v7.3 [58]. For the base case simulation and parametric studies, the gasifier is fed by Illinois#6 coal with the physical and chemical properties listed in Table 3.1. Other coal types that are Coal-A, Coal-B, Coal-Majiri, and Coal-Dilli are used to estimate effects of different coal types on hydrogen production in the system. Their properties are given in Appendix-A.

Table 3.1: Physical and chemical properties of Illinois #6 coal [31, 59]

Proximate analysis	Wt%(as-received)	Wt%(dry)	Ultimate	Wt%(as-received)	Wt%(dry)
Moisture	11.12		Moisture	11.12	
Fixed Carbon	44.19	49.72	Ash	9.7	10.91
Volatiles	34.99	39.37	Carbon	63.75	71.72
Ash	9.7	10.91	Hydrogen	4.5	5.06
Total	100	100	Nitrogen	1.25	1.41
HHV (MJ/kg)	27.13511	30.53107	Chlorine	0.29	0.33
LHV (MJ/kg)	25.88		Sulfur	2.51	2.82
			Oxygen	6.88	7.75

Sulfur analysis in Illinois #6 Coal			
Sulfur Type	Pyritic	Sulfate	Organic
Dry Basis, wt %	1.7	0.02	1.1

Table 3.2: The input parameters of the system

Gasifier, Coal Handling, ASU		Ref.
Carbon conversion, %	98	[60]
Gasifier heat loss, %	1 % of the HHV of the input coal	[61]
Coal preparation power consumption	0.5 % of the HHV of the coal	[62]
Water-slurry %	63	[28]
Gasifier Temperature, ^{0}C	1371	[63]
Gasifier Pressure, bar	42.4	[64]
Radiant cooler temperature, ^{0}C	815.5	[64]
Convective cooler temperature, ^{0}C	260	
Syngas output pressure from convective cooler, bar	41.57	[64]
O_2 purity, %vol	95	[35]
Ratio of O_2 inlet pressure to gasifier, to the gasifier pressure	1.2	[29]
Pressure of O_2 and N_2 delivered by ASU, bar	1.5	[43]
Scrubber		
Scrubber temperature, ^{0}C	220	
Syngas pressure loss, %	1	[35]
NH_3 and HCl percentage of removal	100	[65]
WGS Reactors		
Heat loss from WGS reactors	0%	[60]
Pressure drop for each reactor, bar	0.7	[60]
High temperature reactor COS conversion, %	98	[60]
High temperature reactor approach temperature, ^{0}C	25	[61]
Low temperature reactor approach temperature, ^{0}C	10	[61]
Sulfur removal and CO_2 removal and capturing		
Effectiveness of H_2S removal, %	100	
H2S removal thermal energy consumption, kWh/kgH_2S	5.82	[63]
Syngas pressure loss in H_2S removal, %	1	[35]
Syngas inlet temperature to CO_2 absorption tower, ^{0}C	21	[51]
Pressure in the flash vessels, bar	15/10/3.25/1.05	
Power recovery turbine efficiency, %	77	[52]

CO_2 final delivery pressure, bar	153	[61]
CO_2 compressor isentropic efficiency, %	85	[61]
CO_2 compressor intercooler temperature, ^0C	30	[61]
Syngas Turbine		
Isentropic efficiency, %	85	
PSA unit		
Hydrogen content in the hydrogen product, %	100	
Effectiveness of H_2 separation, %	85	[35]
Purge gas pressure, bar	1.5	[38]
Hydrogen product pressure, bar	20	
Steam cycle		
Heat loss from HRSG, turbines, and pumps	0%	
Steam turbine isentropic efficiency, %	85	
Hydraulic efficiency of pumps, %	75	[35]
Dearator pressure, bar	4	
Max steam cycle temperature, ^0C	565	[35]
Pressure levels, bar	130/40/4/1.5	
Condenser pressure, bar	0.05	[67]
Purge Gas Combustor		
Heat loss from combustor	0%	
Operating pressure, bar	1.5	
Combustor air consumption	20 % above stoichiometric	
Alkaline Electrolyzer		[55]
Rate of hydrogen production, Nm^3/h	485	
Energy required for electrolyzer, kWh/Nm^3	4.3	
Operating temperature, ^0C	80	
Operating pressure, bar	1.034	
Water conversion efficiency, %	80	

The input parameters employed to simulate the system are listed in Table 3.2. These parameters are used for all coals; however, the hydrogen recovery is assumed for 0.85 for Coal Illinois#6, Coal-Dilli, and Coal-B while it is assumed for 0.75 for Coal-A and Coal-Majiri. Hot flue gas heat capacity is estimated very low for 0.85 hydrogen recovery in the PSA for Coal-A and Coal-Majiri, so it is assumed for 0.75.

The information about physical property methods and the modeling of the components in the Aspen Plus is given in this chapter.

3.2 Physical Property Methods

The properties such as enthalpy and entropy were transferred from Aspen Plus to Excel spreadsheet to perform energy and exergy analyses of the system. Choosing correct physical property methods is very important to estimate accurately physical properties in a simulation program.

The HCOALGEN and the DCOALIGT models were used to calculate the enthalpy and density of coal and ash [68]. In this system, the steam cycle was simulated using STEAMNBS physical property method [29, 69]. The simulation of the CO_2 removal unit was also performed using the PC-SAFT equation of state (EOS) [70]. The physical properties of the gasification and downstream unit operations were estimated using the Peng-Robinson EOS with Boston-Mathias alpha function (PR-BM) [71].

3.3 Subsections Simulation

3.3.1 Gasifier

To simulate the gasifier section in the simulation, unit operation blocks that are RYield reactor, RGibbs reactor, coolers, and separator are used in Aspen Plus.

Coal is modeled as a solid in the simulation, it consists of several components. RYield reactor is used to virtually decompose coal its various components. This reactor is a prerequisite step for coal gasification.

Coal gasification is simulated using an RGibbs reactor. RGibbs reactor is an equilibrium reactor. Chemical reactions can be simulated using this reactor in two ways. One method is that possible products are defined and Gibbs free energy minimization method is used to obtain products. Another method is that an independent set of chemical reactions can be used in the reactor. For this method, one or more chemical reactions can be specified with approach temperature. Approach temperature shows the difference between the reactor temperature and the equilibrium temperature of the reaction. Independent chemical reactions are used in this study. Chemical reactions are given in below [61]:

$H_2O + CO \rightarrow CO_2 + H_2$ (3.1)

$C + 0.5O_2 \rightarrow CO$ (3.2)

$C + O_2 \rightarrow CO_2$ (3.3)

$Cl_2 + H_2 \rightarrow 2HCl$ (3.4)

$N_2 + 3H_2 \rightarrow 2NH_3$ (3.5)

$CH_4 + H_2O \rightarrow CO + 3H_2$ (3.6)

$S + H_2 \rightarrow H_2S$ (3.7)

$CO + S \rightarrow COS$ (3.8)

All of the reactions in the gasifier are assumed at chemical equilibrium at gasifier temperature except water gas shift reaction [61, 72]. Approach temperature is assumed at -200℃ for water gas shift reaction (Eq.3.1) [61]. Heat loss from the gasifier is calculated using FORTRAN in Aspen Plus.

Heat from radiant and convective cooler are calculated using cooler in the simulator. To calculate the heat capacity of the syngas coolers, streams temperature that enter and exit to the syngas coolers are defined; in addition to the temperature pressure drop is also defined. A separator block is used to separate slag from the raw syngas after the radiant cooler.

3.3.2 Scrubber

Separator block in Aspen Plus is employed for simulation of the scrubber. It is assumed that all of the HCl and NH_3 are removed in the scrubber [65].

3.3.3 Air Separation Unit

A purity of 95% oxygen is produced by the ASU for the coal gasification process. The ASU is modeled in the Aspen Plus using two multistage compressors, and a separator block. Air pressure increases in the first multistage compressor to separate oxygen and nitrogen in the ASU. Then oxygen pressure that is produced in the ASU increases to 1.2 times the gasifier pressure in the second multistage compressor. The amount of oxygen is specified as a design specification in the simulation to control the gasifier temperature.

3.3.4 Water Gas Shift Reactors

REQUIL reactor is used for modeling of the WGS reactors. This reactor calculates chemical equilibrium for specified chemical reactions. Conversion of CO to CO_2 and conversion of COS to H_2S take place in the WGS reactors. It is assumed that 98% of COS is converted to H_2S [60]. This conversion ratio is specified as a design specification in Aspen Plus. The reactions take place in the WGS reactors are shown below:

$$CO + H_2O \leftrightarrow CO_2 + H_2 \quad (3.9)$$

$$COS + H_2O \leftrightarrow CO_2 + H_2S \quad (3.10)$$

25℃ and 10℃ approach temperatures for water gas shift reaction (Eq.3.9) are used for high temperature and low temperature in the REQIL reactors for high and low temperature WGS reactors, respectively [61]. The reactors are assumed adiabatic. Steam has been injected to the high temperature WGS reactor from the steam cycle to achieve a 2:1 molar ratio for H_2O-CO. The amount of injected steam is set using design specification in Aspen Plus. Two coolers are used for heat recovery from the WGS reactors.

3.3.5 Acid Gas Removal

Power consumption of the H_2S removal and CO_2 removal and capturing units are considered for the simulation of the acid gas removal unit in the system.

H_2S removal unit is not simulated in detail. Indeed, the separator block with some simplifications is employed to simulate H_2S removal because power consumption of the H_2S removal is very low and to simplify the system simulation. The CO_2 removing and capturing is modeled in detail based on the system explained in Ref. [51]. CO_2 removal unit is simulated to estimate the power that is necessary to remove 1 (kmol/s) CO_2. Then this estimation is used for

parametric studies. To estimate physical properties of the Selexol and streams in the CO_2 removal unit, Ref. [70] is used. CO_2 removal efficiency is defined as follows:

$$CO_2 \text{ removal efficiency} = \frac{n_{feed,CO2} - n_{clnsyn,CO2}}{n_{feed,CO2}} \quad (3.11)$$

In this equation, $n_{feed,CO2}$ shows the mole number of CO_2 in the stream that enters the CO_2 removal unit, and $n_{clnsyn,CO2}$ shows the mole number of CO_2 in the clean syngas. Flow rate of the Selexol is specified as a design specification in Aspen Plus to remove certain amount of CO_2. Two hydraulic turbines are used to decrease power requirement of the CO_2 removal unit. Mechanical efficiency of the turbines is assumed as 77% [52].

3.3.6 Pressure Swing Adsorption

PSA is modeled using a separator block. H_2 recovery efficiency, pressure of the purge gas, and pressure of the recovered H_2 are specified in the separator block. Recovered H_2 pressure and temperature are assumed as same pressure and temperature of the stream that enters into the PSA. Purge gas pressure is assumed at 1.5 bars and the temperature at feed stream temperature. All of the assumptions based on manufacturer data [54]. Hydrogen recovery efficiency of the PSA is defined in the below equation:

$$H_2 \text{ recovery efficiency} = \frac{n_{clnsyn,H2} - n_{H2}}{n_{clnsyn,H2}} \quad (3.12)$$

where $n_{clnsyn,H2}$ shows the mole number of H_2 in the fed stream to PSA, and n_{H2} shows the mole number of recovered H_2 in the PSA.

3.3.7 Combustor

Purge gas, steam, and air react in the combustor. RGibbs reactor is used for simulation of the combustor. Possible products are defined and mole numbers of the products are estimated using Gibbs free energy minimization method in the reactor. It is assumed that the combustor is adiabatic and pressure drops in the reactor is negligible. 20% above stoichiometric air is used for combustion process. The amount of air is set up using FORTRAN in Aspen Plus. The flue gas that enters the HRSG is controlled at 800℃ by mixing air and hot flue gas. The amount of mixing air is determined as a design specification. Air compressor is used in the simulation to increase atmospheric air pressure to combustor pressure.

3.3.8 Heat Recovery Steam Generator and Power Generation

MHEATX block in Aspen Plus is employed as a HRSG to recovery heat from the hot flue gas. Heat transfer between multiple hot and cold streams can take place in MHEATX block with rigorous internal zone analysis. 5℃ or greater approach temperature is assumed in the MHEATX block. Stack gas is assumed saturated vapor. Calculator and transfer blocks are used to produce steam using available heat from radiant, convective, and WGS reactors coolers. Steam requirement of different subsections are considered to determine pressure levels of the steam cycle. Turbine subroutine with 85% isentropic efficiency is used to estimate power production from the steam cycle.

3.3.9 Water Electrolyzer

Simulation of the alkaline water electrolyzer is performed using a RSTOIC reactor and a separator block in the simulator. First power consumption of the components such as ASU, CO_2 removal and capturing are calculated in the Calculator block using FORTRAN in Aspen Plus. Then, remaining power is calculated to produce extra hydrogen in the alkaline water electrolyzer. Finally, the flow rate of the water that enters the electrolyzer is estimated.

In the RSTOIC reactor, water is converted to H_2 and O_2. Water conversion efficiency is assumed as 80%. All of the assumptions that are used for the simulation of the alkaline water electrolyzer based on Ref. [55]. The following reactions take place in the RSTOIC reactor:

$$H_2O \rightarrow 0.8H_2 + 0.5O_2 + 0.2H_2O \quad (3.13)$$

After the RSTOIC reactor, H_2, O_2, and unconverted water are separated to three different streams in the separator block.

Chapter 4
Thermodynamic Modeling

4.1 Overview

Overall system energy efficiency, exergy efficiency, and the gasifier cold gas efficiency are calculated using thermodynamic first and second laws. In addition, an exergy analysis is performed to find the exergy destructions and exergy efficiencies of the components in the system. Physical properties and mass flow rates of the streams that are used in the exergy analysis are transferred from Aspen Plus to Excel spreadsheet.

4.2 Efficiency Analysis

The overall system efficiency is defined by the ratio of the total lower heating value (LHV) of the produced hydrogen to LHV of the input coal. The overall system exergy efficiency is also estimated by the ratio of the produced hydrogen exergy to input coal exergy. The following equations are used to find the overall energy and exergy efficiencies of the system:

$$\eta_{en,system} = \frac{(\dot{m}_{H_2,electrolyzer} + \dot{m}_{H_2,PSA}) \times LHV_{H_2}}{\dot{m}_{coal} \times LHV_{coal}} \quad (4.1)$$

$$\eta_{ex,system} = \frac{(\dot{m}_{H_2,electrolyzer} + \dot{m}_{H_2,PSA}) \times ex_{H_2}}{\dot{m}_{coal} \times ex_{coal}} \quad (4.2)$$

where $\dot{m}_{H_2,PSA}$ shows hydrogen production rate from the PSA unit and $\dot{m}_{H_2,electrolyzer}$ is hydrogen production rate from the electrolyzer.

Cold gas efficiency is also important for the system analysis. It measures of the gasifier performance. Cold gas efficiency can be defined as follows:

$$\eta_{cg,gasifier} = \frac{(LHV_{H_2} \times \dot{m}_{H_2,syngas}) + (LHV_{CO} \times \dot{m}_{CO,syngas}) + (LHV_{CH_4} \times \dot{m}_{CH_4,syngas})}{\dot{m}_{coal} \times LHV_{coal}} \quad (4.3)$$

where $\dot{m}_{H_2,syngas}, \dot{m}_{CO,syngas}$, and $\dot{m}_{CH_4,syngas}$ show the mass flow rate of H_2, CO, and CH_4 in the syngas.

4.3 Exergy Analysis

Here, the chemical exergy values of each stream are estimated from the standard chemical exergies of the substances. Standard chemical exergy values of the required substances at 25 ^{o}C and 1 atm are listed in Table 4.1.

Table 4.1: Standard chemical exergy values of different components [73]

Substance	Standard chemical exergy (kJ/mol)
CO	274.71
CO_2	19.48
H_2	236.09
H_2O (l)	0.9
H_2O(g)	9.5
N_2	0.72
CH_4	831.2
H_2S	812
HCL	84.5
O_2	3.97

The specific chemical exergy of gas mixtures can be calculated as

$$ex_{ch} = \Sigma y_i ex_{ch,i} + RT_o \Sigma y_i \ln y_i \quad (4.4)$$

The chemical exergy of the coal is written as [74]:

$$ex_{ch}^{coal} = \left[(CCV^o + w \times h_{fg})\beta + 9417s\right] \quad (4.5)$$

where

$$\beta = 0.1882\frac{h}{c} + 0.061\frac{o}{c} + 0.0404\frac{n}{c} + 1.0437 \quad (4.6)$$

Here, CCV^o is the net calorific value of the coal, w is the moisture content of the coal, h_{fg} is the latent heat of water at T_0, and s, c, h, o, n are the mass fraction of sulfur, carbon, hydrogen, oxygen, and nitrogen in the coal, respectively.

In this study, total exergy of each stream is determined from summation of the physical and chemical exergies. The variations of kinetic and potential exergies are assumed to be negligible. The specific physical exergy is given as

$$ex_{ph,i} = (h_i - h_0) - T_0(s_i - s_0) \quad (4.7)$$

The exergy destruction and exergy efficiency of turbines and compressors are determined from the following equations [75, 76]:

$$\dot{E}x_D^T = -\dot{W}_T + [\dot{E}x_{in} - \dot{E}x_{out}] \quad (4.8)$$

$$\dot{E}x_D^C = \dot{W}_C + [\dot{E}x_{in} - \dot{E}x_{out}] \quad (4.9)$$

$$\eta_{ex}^T = \frac{\dot{W}_T}{\dot{E}x_{in,T} - \dot{E}x_{out,T}} \quad (4.10)$$

$$\eta_{ex}^C = \frac{\dot{E}x_{out,C} - \dot{E}x_{in,C}}{\dot{W}_C} \quad (4.11)$$

The exergy destruction in the water electrolyzer is obtained using Gibbs free energy equation. First, the minimum work requirement is determined, and then, the difference between the minimum work requirement and the actual work is considered as the electrolyzer exergy destruction. The exergy efficiency of the electrolyzer is defined as the ratio of the minimum work requirement to the actual work. The minimum work requirement, exergy destruction and exergy efficiency of the electrolyzer are written as follows [77, 78]:

$$\dot{W}_{rev} = \Delta G(T) = \Delta H(T) - T\Delta S(T) \tag{4.12}$$

$$\Delta H(T) = \Delta H^{o}_{298.15} + \int_{298.15}^{T} c_p \, dT \tag{4.13}$$

$$\Delta S(T) = S^{o}_{298.15} + \int_{298.15}^{T} \frac{c_p}{T} dT \tag{4.14}$$

and

$$\dot{Ex}_{D}^{Electrolyzer} = \dot{W}_{act} - \dot{W}_{rev} \tag{4.15}$$

as well as

$$\eta_{ex}^{Electrolyzer} = \frac{\dot{W}_{rev}}{\dot{W}_{act}} \tag{4.16}$$

The method used to define the exergy destruction and efficiency of the electrolyzer is employed for exergy analysis of the ASU and CO_2 removal unit. The minimum work requirement for both ASU and CO_2 removal unit can be calculated as

$$\dot{W}_{min} = \Delta G_{sep} = \Delta G_B + \Delta G_C - \Delta G_A \tag{4.17}$$

where A is the stream that enters the separation unit, B is the oxygen rich stream for the air separation unit and carbon dioxide rich stream for the CO_2 removal unit, and C is the vent gases form the air separation unit and clean syngas for the CO_2 removal unit. The streams are shown in Figure 4.2 for CO_2 removal.

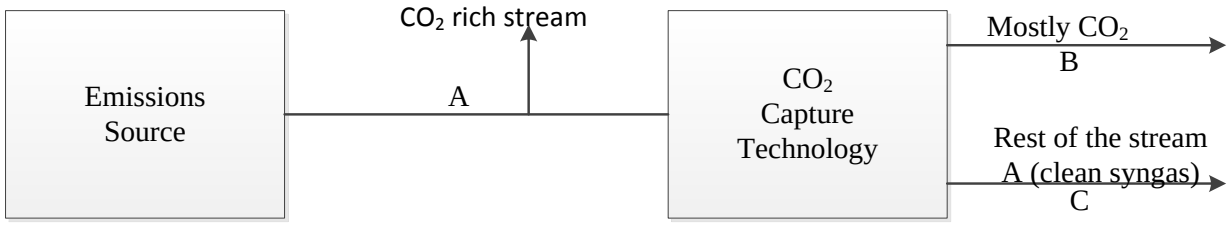

Figure 4.1: Schematic of carbon removal (Adapted from [79])

The exergy destructions of the ASU and CO_2 removing and capturing unit are obtained from

$$\dot{E}x_D^{ASU} = \dot{W}_{act}^{ASU} - \dot{W}_{min}^{ASU} \quad (4.18)$$

$$\dot{E}x_D^{CO2rcu} = \dot{W}_{act}^{CO2cru} - \dot{W}_{min}^{CO2cru} \quad (4.19)$$

Note that the exergy destruction and efficiency of pumps are determined from Eqs. (4.9) and (4.11) by consideration of the actual pump work instead of the compressor work. The exergy destruction and exergy efficiency of the other system components are in general written as follows:

$$\dot{E}x_D = \Sigma\dot{E}x_{in} - \Sigma\dot{E}x_{out} \quad (4.20)$$

$$\eta_{ex} = \Sigma\dot{E}x_{out}/\Sigma\dot{E}x_{in} \quad (4.21)$$

The exergy destruction ratio [80] for each component is also calculated by

$$Y_D = \left(\dot{E}x_D\right)x/\Sigma\dot{E}x_{F,tot} \quad (4.22)$$

Chapter 5
Results and Discussion

5.1 Energy and Exergy Analysis Results

The composition, temperature, and pressure of the main streams in the system studied were determined and listed in Table 5.1. As indicated in this table, stream#3, which is the syngas stream gasifier exit, has the main gaseous components of CO, CO_2, H_2, and H_2O. The flow rate of water in stream#8, which is the water utilized in the high – temperature WGS reactor to achieve a 2:1 molar ratio of H_2O: CO, was estimated to be ~1.87 kmol/s. In practice, this flow rate should be a little different. To achieve more accurate flow rate for stream#8, it is necessary to model the scrubber unit in detail. Of course, the improvement in prediction of this flow rate does not significantly affect the system performance.

Table 5.2 summarizes the power production and consumption, hydrogen production, and emission performance of the system studied. The simulation results indicated that 79.3 MW and 3.5 MW power are produced in the steam and syngas turbines, respectively, and the total power production in the system is ~83 MW. From this power, ~57 MW is utilized in different power consumers in the system. Among different power consumers, the air separation unit has the highest potential with ~23 MW, followed the CO_2 removal and capturing unit and O_2 compressor with 16.4 MW and 9.4 MW, respectively. Around 26 MW of the total power production in the system is used for extra hydrogen production in an alkaline water electrolyzer. The rate of this hydrogen production is ~543 kg/h, which is ~4% of the total hydrogen production in this system. Of course, it is possible to increase the rate of this hydrogen production if a high temperature steam electrolyzer is employed instead of the alkaline water electrolyzer.

Table 5.1: Streams results in the system studied

Streams	Coal	Slurry water	2	3	4	5	6	7	8	9	10	11	12	13
Mole Fractions y(i)														
CO				0.39	0.39	0.39	0.39	0.39		0.051	0.051	0.782E-2	0.782E-2	
CO_2				0.104	0.104	0.104	0.104	0.105		0.26	0.26	0.304	0.304	
H_2				0.295	0.295	0.295	0.295	0.297		0.38	0.38	0.434	0.434	
H_2O				0.185	0.185	0.185	0.185	0.186	1	0.296	0.296	0.253	0.253	1
N_2			0.017	0.008	0.008	0.008	0.008	0.008		0.543E-2	0.543E-2	0.543E-2	0.543E-2	
AR			0.0318	0.007	0.007	0.007	0.007	0.007		0.493E-2	0.493E-2	0.493E-2	0.493E-2	
CH_4				8.75E-5	8.75E-5	8.75E-5	8.75E-5	8.82E-5		5.51E-5	5.51E-5	5.51E-5	5.51E-5	
H_2S				0.007	0.007	0.007	0.007	0.007		0.258E-3	0.258E-3	0.258E-3	0.258E-3	
O_2			0.95	2.04E-12	2.04E-12	2.04E-12	2.04E-12	2.05E-12		1.28E-12	1.28E-12	1.28E-12	1.28E-12	
HCL				0.788E-3	0.788E-3	0.788E-3	0.788E-3							
NO				9.81E-13	9.81E-13	9.81E-13	9.81E-13	9.88E-13		6.18E-13	6.18E-13	6.18E-13	6.18E-13	
Total (kmol/sec)	30 kg/sec	0.684	0.776	3.15	3.15	3.15	3.15	3.126	1.87	5.001	5.001	5.001	5.001	5.392
T(K)	298.15	333.15	408.32	1644.15	1088.7	1088.7	533.15	493.15	554	714.3	483.15	528.47	312.15	302.14
P(kPa)	4481.6	4481.6	5088.33	4240.27	4226.48	4226.48	4157.54	4115.96	4000	3930	3930	3860	3860	400
Vapor Fraction	Solid	0	1	1	1	1	1	1	1	1	1	1	0.747	0

Streams	14	15	16	17	18	19	20	21	22	23	24	25	26	27
Mole Fractions y(i)														
CO												0.104E-1	0.165E-1	0.165E-1
CO_2												0.407	0.646E-1	0.646E-1
H_2												0.568	0.899	0.899
H_2O	1	1	1	1	1	1	1	1	1	1	1			
N_2												0.728E-2	0.115E-1	0.115E-1
AR												0.66E-2	0.72E-2	0.72E-2
CH_4												7.38E-5	0.114E-3	0.114E-3
O_2												1.72E-12		
NO												8.28E-13		
Total (kmol/sec)	5.392	1.212	4.18	4.18	4.18	0.232	3.42	3.42	3.42	3.42	3.42	3.733	2.352	2.352
T(K)	416.79	416.79	416.79	417.47	523.54	523.54	523.54	526.66	604.03	604.03	734.95	312.15	359	308.253
P(kPa)	400	400	400	4000	4000	4000	4000	13000	13000	13000	13000	3860	3800	2000
Vapor Fraction	0.225	1	0	0	0.055	1	0	0	0	1	1	1	1	1

Streams	28	29	30	31	32	33	36	39	41	Hot flue gas	42	43	44	45	46	Stack
Mole Fractions y(i)																
CO	0.072									1.17E-7						1.17E-7
CO_2	0.284									0.052						0.052
H_2	0.592									4.56E-7						4.56E-7
H_2O		1				1	1	1	1	0.388	1	1	1	1	1	0.388
N_2	0.05		0.79	0.79	0.79					0.482						0.482
CH_4	4.9E-4									5.42E-30						5.42E-30
O_2			0.21	0.21	0.21					0.0775						0.0775
NO										6.29E-5						6.29E-5
Total (kmol/sec)	0.535	1.11	2.205	1.015	1.2	0.526	0.0936	1.545	1.545	3.672	0.526	0.232	1.212	0.607	0.607	3.672
T(K)	308.15	495.4	339.6	339.6	339.6	523.54	353.15	664.65	838.15	1073.15	838.15	838.15	547.4	302.5	450.6	359.92
P(kPa)	150	150	150	150	150	4000	103.4	4000	4000	150	4000	4000	400	150	150	150
Vapor Fraction	1	1	1	1	1	0	0	1	1	1	1	1	1	0	1	1

Table 5.2: Power production and consumption, system efficiency, hydrogen production, and emission performance of the system

Power Production and Consumption (MW)	
Auxiliary power consumption	-5.45
ASU	-23
O_2 compressor	-9.44
CO_2 removal	-7.5
CO_2 capturing	-8.64
Air compressor (air for combustor)	-2.66
Steam Turbine	79.35
Syngas Turbine	3.52
Electrolyzer unit	-26.1
Net power production	0
System Efficiency	
Exergy efficiency of the system, %	55.7
Energy efficiency of the system, %	58.4
Hydrogen Production (kg/h)	
Hydrogen production from PSA	13058.64
Hydrogen production from electrolyzer	543.44
Total hydrogen production	13602.08
Emissions Performance (kg/h)	
CO emissions	0.043
CO_2 emissions	30280.8
NO_x emissions	24.97
Captured CO_2	217008

It is noted that the rate of hydrogen production in the PSA unit is 13,058 kg/h; and the total hydrogen production in this system from 108,000 kg/h input coal is 13,602 kg/h. Thus, the weight ratio of the hydrogen yielded to the coal fed to this system is ~0.126 and the system overall energy efficiency is ~58.4%. Although this system produces hydrogen from coal, the system produced greenhouse gases are not high. This is because of ~217,008 kg/h CO_2 captured in this system. Indeed, this system produces only ~0.043 kg/h CO, ~30280 kg/h CO_2, and ~24.97 kg/h NO_x. Of course, the NO_x production can be eliminated or reduced if more steam is used during the purge gas combustion process. In this study, it was assumed that the effectiveness of the H_2S removal unit is ideal as 100%. In practice, there will be a little amount of SO_x in the exit flue gas from this system.

The exergy destruction ratio indicates the ratio of exergy destruction in a system component to the entrance fuel exergy to the system. As seen in Figure 5.1, the highest exergy destruction takes place in the gasifier with an exergy destruction ratio of ~18%. The main reason for this high exergy destruction is the irreversibilities due to chemical reactions in the gasifier. Other significant exergy destructions occur in the combustor with 7.3%, ASU with 2.4%, radiant cooler with 2.0%, high-temperature WGS reactor with 1.8%, steam turbine 1.6%, and HRSG with 1.3%. The ratio of exergy destructions for the other components is less than 1%. The exergy efficiency of the system components is also shown in Figure 5.2. As seen in this figure, the radiant cooler exergy efficiency becomes ~67% which is exergetically less efficient than the other heat transfer processes in the system. The reason of that is the high temperature difference during the heat transfer process. The lowest exergy efficiencies appear to be for the air separation unit and the combustor as 17% and 57%, respectively. The main reason of such a low exergy efficiency of the air separation unit is the irreversibilities occurred during the compression process. For combustor, the reason is the chemical reactions happened in the combustor. The results revealed that the overall exergy efficiency of this system is 55.7%. This efficiency can be improved if the heat transfer in the radiant cooler takes place outside the gasifier. In this condition, the temperature difference during the heat transfer process decreases [36].

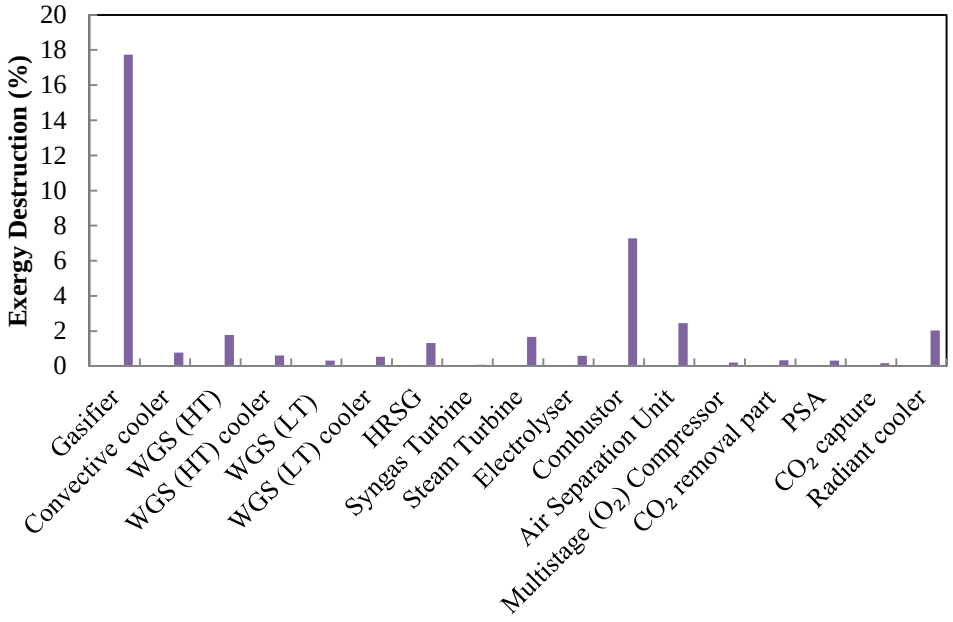

Figure 5.1: Exergy destructions in the system components as a percentage of the fuel total exergy

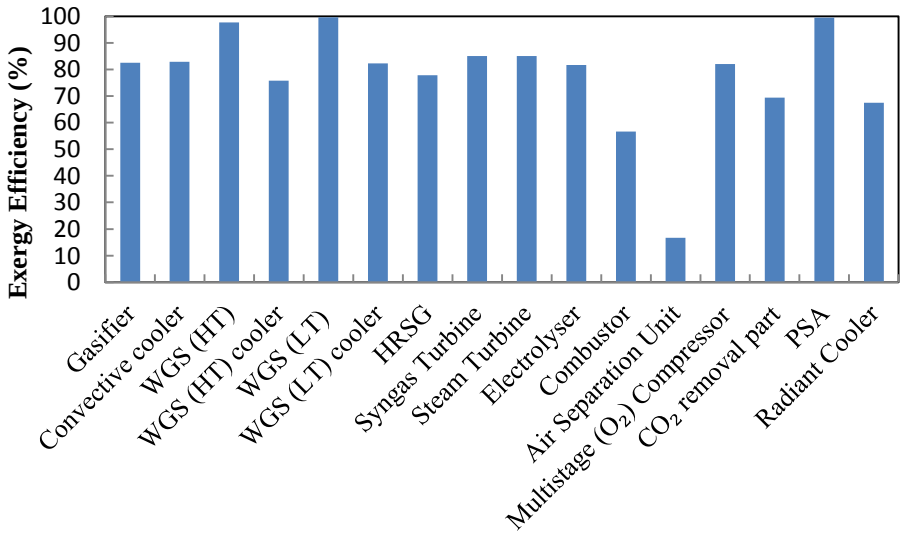

Figure 5.2: Exergy efficiencies of the system components

5.2 Parametric Study Results

To estimate the effect of the effectiveness of CO_2 removal unit, H_2 recovery in the PSA unit, water ratio in the coal slurry, and the gasifier temperature on the rate of hydrogen production in the system, a parametric study was performed. The variations of exergy destruction and exergy efficiency of the gasifier were also calculated by changing the water ratio in the slurry and the gasifier temperature. For all the cases considered, the gasifier heat loss is assumed to be the same as the base case, and the gasifier temperature is controlled by changing the inlet oxygen flow rate to the gasifier. The gasifier temperature is also the same as the base case for the first three parameters mentioned above. The PSA hydrogen recovery is assumed to be constant once the effectiveness of the CO_2 removal unit varies.

The effect of the effectiveness of the CO_2 removal on the hydrogen production is shown in Figure 5.3. The rate of hydrogen production increases ~170 kg/h with decreasing CO_2 removal from 0.9 to 0.5. Since CO_2 removal and capturing processes need lower power requirement, the hydrogen production from the electrolyzer increases. However, this situation causes higher CO_2 emissions, so it does not seem a good idea for this increase. The effect of the PSA unit hydrogen recovery on the system hydrogen production is demonstrated in Figure 5.4. As it is expected, hydrogen production of the electrolyzer increases with decreasing hydrogen recovery from the PSA unit. The results indicated that ~1000 kg/h hydrogen is produced from the electrolyzer if the hydrogen recovery of the PSA unit is 0.7, while only ~360 kg/h hydrogen is produced if the PSA unit hydrogen recovery is 0.9. Although the production of the electrolyzer significantly increases, the total hydrogen production decreases with decreasing the PSA unit hydrogen

recovery. The highest total hydrogen production is 1490 kg/h for 0.9 hydrogen recovery. A lower hydrogen recovery may be suitable for hydrogen and electricity co-generation.

The variation of the hydrogen production with the change of the water ratio in the coal slurry is demonstrated in Figure 5.5. As shown in the figure, the rate of hydrogen production from the electrolyzer rises from ~543 to ~807 kg/h with an increase in the water ratio in the coal slurry; however, total hydrogen production decreases from ~13050 to ~12360 kg/h due to decrease of the hydrogen production in the PSA unit. The radiant cooler and convective cooler heat capacity increase with higher water ratio in coal slurry; thus, more power is obtained for the electrolyzer. The exergy destruction and exergy efficiency of the gasifier are shown in Figure 5.6. The exergy destruction and exergy efficiency decrease with an increase in the water ratio in the coal slurry. The reason is that more energy is required for water vaporization that reduces the syngas yield. If this ratio increases from 0.41 to 0.59, the exergy destruction increases almost 7.5% and the exergy efficiency decreases almost 1.5%, respectively.

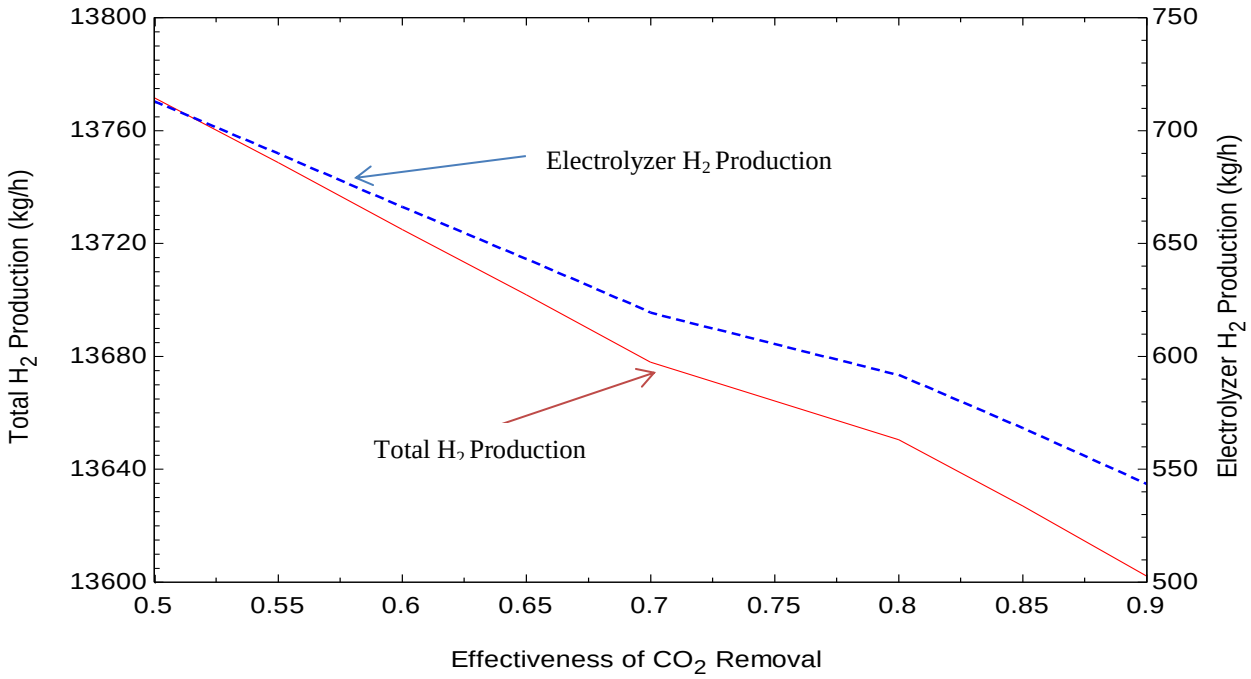

Figure 5.3: The effectiveness of the CO_2 removal unit on the rate of the hydrogen production

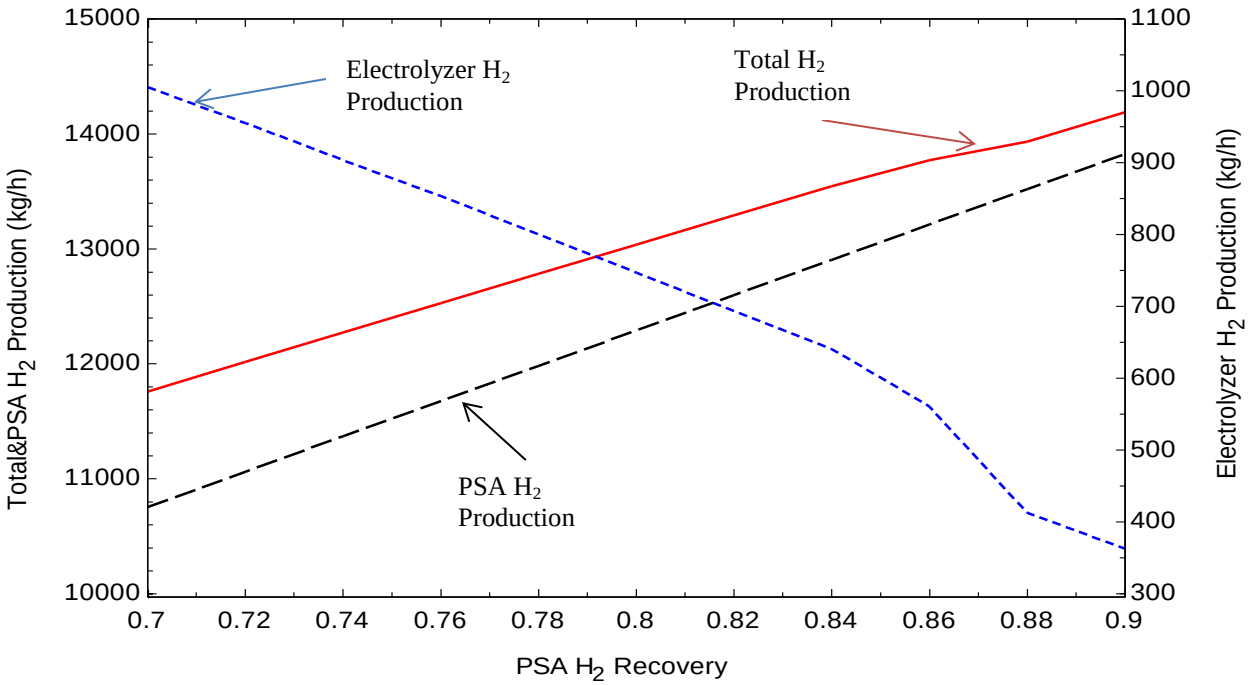

Figure 5.4: The effect of the hydrogen recovery in the PSA unit on the rate of the hydrogen production

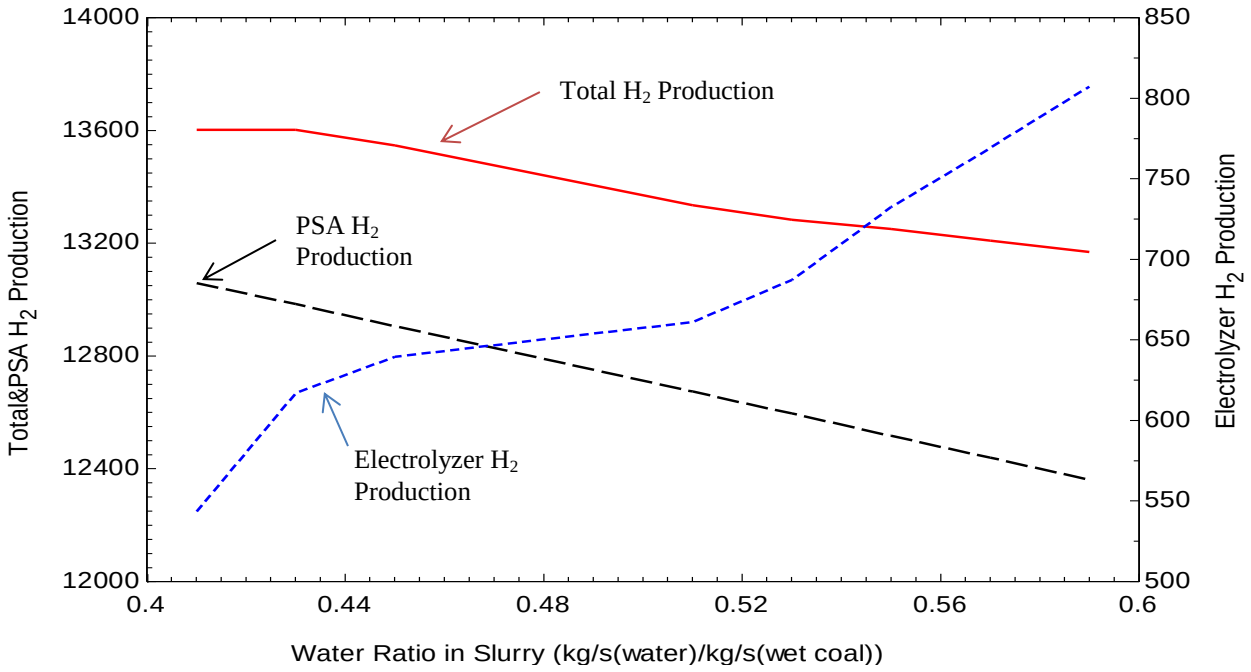

Figure 5.5: The effect of the water-coal ratio in the coal slurry on the rate of the hydrogen production

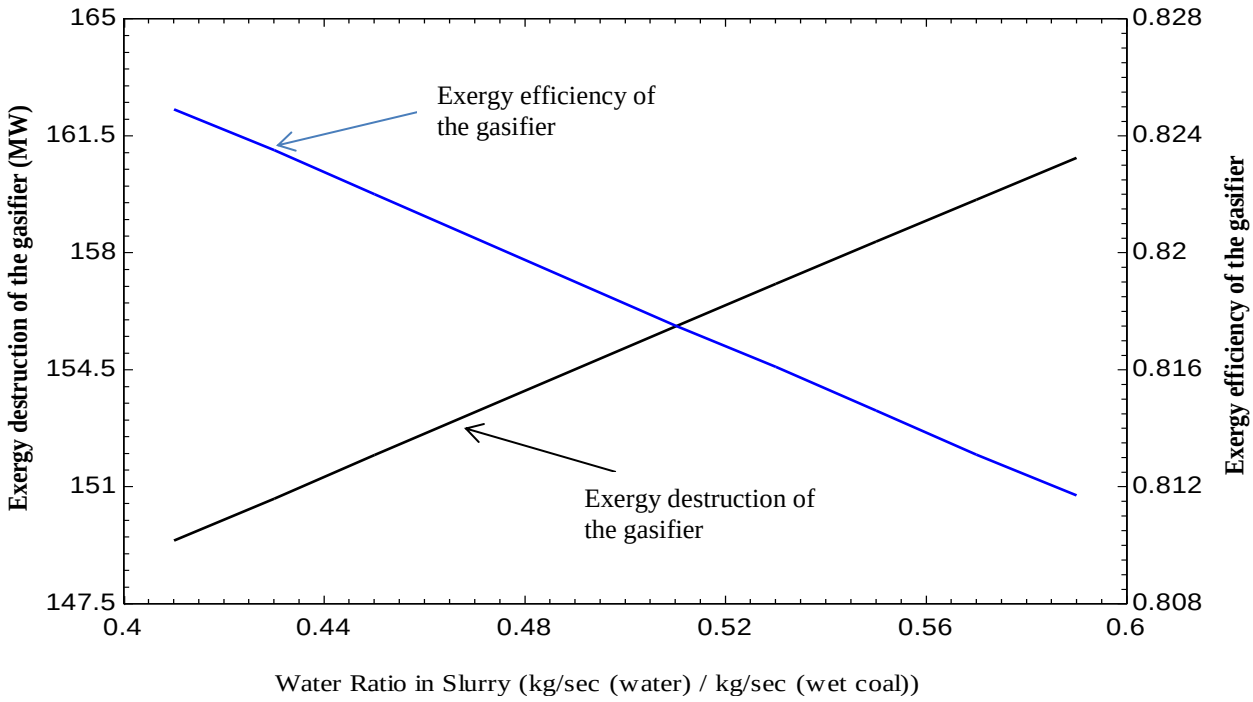

Figure 5.6: The effect of the water-coal ratio in the coal slurry on the exergy destruction and exergy efficiency of the gasifier

As shown in Figure 5.7, total hydrogen production reduces and the hydrogen production from the electrolyzer increases with an increase in the gasifier temperature. By increasing the gasifier temperature, the radiant cooler and convective cooler heat capacity increases and more power is generated in the system; thus the hydrogen production from the electrolyzer increases. However, oxygen requirement for the gasification rises for higher gasifier temperature and coal undergoes combustion rather than gasification. Therefore, the mole fraction of hydrogen in the syngas and total hydrogen production decrease. The hydrogen production from the electrolyzer rises ~30%, hydrogen production from the PSA unit decreases ~2.5%, and the total hydrogen production reduces ~1.3% by varying the gasifier temperature from 1300 ℃ to 1400 ℃. The effects of the gasifier temperature on the gasifier exergy destruction and efficiency are shown in Figure 5.8. Although physical exergy of the syngas increases with an increase the gasifier temperature, the chemical exergy decreases. Therefore, the exergy destruction of the gasifier reduces ~2 MW by increasing the gasifier temperature from 1300 ℃ to 1400 ℃. The exergy efficiency of the gasifier is also reduced by approximately 0.3%.

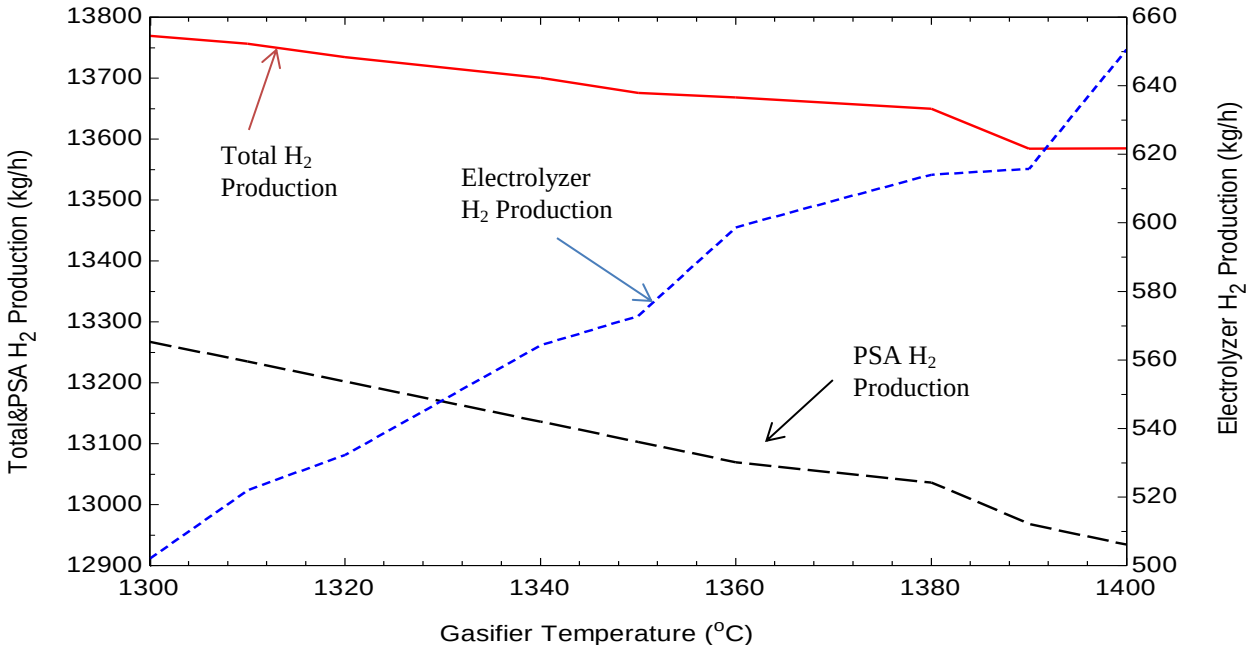

Figure 5.7: The effect of the gasifier temperature on the rate of the hydrogen production

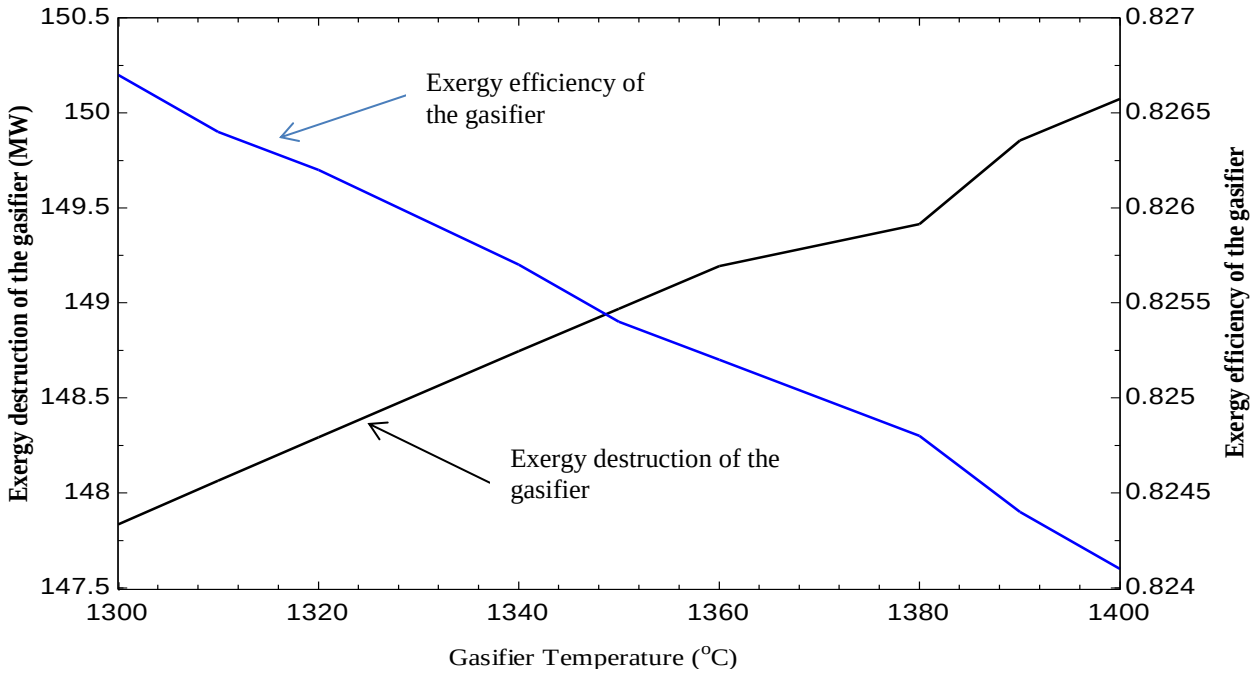

Figure 5.8: The effect of the gasifier temperature on the exergy destruction and exergy efficiency of the gasifier

5.3 Effects of Different Coal Types on the Hydrogen Production

Table 5.3 summarizes the energy and exergy efficiencies, power production and consumption, and emission performance of the system studied for the different types of the coals. As shown in the table, the highest energy and exergy efficiencies are 58.4% and 55.7 % respectively for Coal Illinois, and the lowest being is 45.3% and 41.62% for Coal A. Close energy and exergy efficiencies are obtained using other high ranking coals- B, and Dilli. The efficiencies of coal A; 45.3% and 41.62%, are close to the efficiencies of another low ranking coal Majiri at 47.5% and 44.3%. The simulation results show that the highest power is obtained using Coal B in the system. 80.95 MW and 4.11 MW power are produced in the steam and syngas turbines for Coal B, respectively, and the total power production in the system is ~85 MW. Coal Majiri has 14% less power production than Coal B. The power productions are estimated ~82.8 MW, ~78 MW, and ~78.1 MW, respectively for Coal Illinois, Coal A and Coal Dilli. Although power production from Coal A and Coal Majiri are lower than other coals, the power consumptions of different units such as ASU, CO_2 removal and capturing units are less than the other coals. The air separation unit has the highest power consumption for all of the coal types; however, power consumption of the ASU is ~14.3 MW for Coal Majiri and ~24.5 MW for Coal B. The main reason for this difference is using different amount of oxygen in the gasifier for different types of gasifier. Figure 5.9 indicates oxygen consumption of the coals for per kg of coal. The highest oxygen consumption is equal to ~0.83 O_2 (kg/sec)/Coal (kg/sec) for Coal B, so the highest power consumption in the ASU is estimated for Coal B. Oxygen consumption not only affects power consumption of the ASU, but also affects power consumption of the multistage oxygen compressor. As shown in Table 5.3, power consumption of the multistage compressor for Coal B

is ~41% higher than the power consumption for Coal Majiri. Power consumption of the ASU is equal to ~23 MW for Coal Illinois and ~20.6 MW for Coal Dilli, although these coals consist of close amount of elements. The main reason for that is coal – water slurry for Coal Illinois has lower solids loading due to higher moisture content, so oxygen demand for Coal Illinois is higher than Coal Dilli. This should be considered for cost analysis of the system because cost of the ASU has significant contribution on the system power consumption [21]. CO_2 removal and capturing units are also significant contributors on the system power consumption. The results reveal that there is a direct relationship between carbon content in the coals and power consumption of the CO_2 removal and capturing units. According to the Ultanal analysis, carbon content in Coal A is ~42.5% and ~75.1% for Coal B, thus power consumptions of carbon removal and capturing units for Coal B is ~76.7 higher than Coal A. High carbon content is also significant effects on the CO_2 emissions from the system. The CO_2 emissions for Coal A is equal to ~18880 kg/hr; however, the CO_2 emissions is estimated ~33148 kg/hr for Coal B.

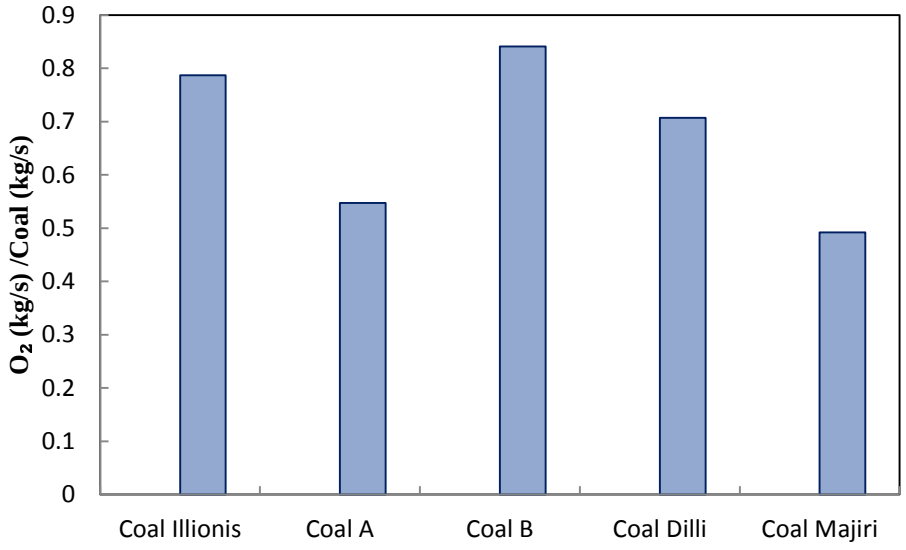

Figure 5.9: Oxygen consumption of the coals for per kg of coal

Table 5.3: The effects of the coals on the system performance

Coal Types	Coal Illinois	Coal A	Coal B	Coal Dilli	Coal Majiri
Power Production and Consumption (MW)					
Auxiliary power consumption	-5.45	-4.48	-5.5	-5.81	-5.73
ASU	-23	-15.99	-24.58	-20.67	-14.38
O2 compressor	-9.44	-6.54	-10.05	-8.45	-5.88
CO2 removal	-7.5	-4.63	-8.18	-7.5	-4.84
CO2 capturing	-8.64	-5.33	-9.42	-8.16	-5.57
Air compressor (air for combustor)	-2.66	-3.07	-3.31	-2.3	-2.38
Steam Turbine	79.35	76.01	80.95	79.35	71.6
Syngas Turbine	3.52	2.02	4.11	3.52	2.03
Electrolyzer unit	-26.1	-37.98	-24	-26.1	-34.83
Net power production	0	0	0	0	0
System Efficiency					
Exergy efficiency of the system, %	55.7	41.62	54.65	51.76	44.33
Energy efficiency of the system, %	58.4	45.36	57.51	55	47.5
Emissions Performance (kg/hr)					
CO emissions	0.043	0.07	0.12	0.02	0.021
CO2 emissions	30280.8	18880.88	33148.33	28569.32	19542.54
NOx emissions	24.97	37.25	39.5	18.11	20.87
Captured CO2	217008	133903.4	236519.35	205204.35	140074.7

The effect of using different types of coal on the cold gas efficiency on the gasifier is shown in the Figure 5.10. As shown in the figure, the gasifier cold gas efficiency is around 70% for high ranking coals. However, the cold gas efficiency is estimated ~60% for Coal A, and ~63% for Coal Majiri. The highest cold gas efficiency is obtained using Coal Illinois, and it is ~18.7% higher than the cold gas efficiency of the gasifier that Coal A is used. To improve cold gas efficiency of the gasifier, coal – CO_2 slurry feed can be used instead of coal – water slurry [28].

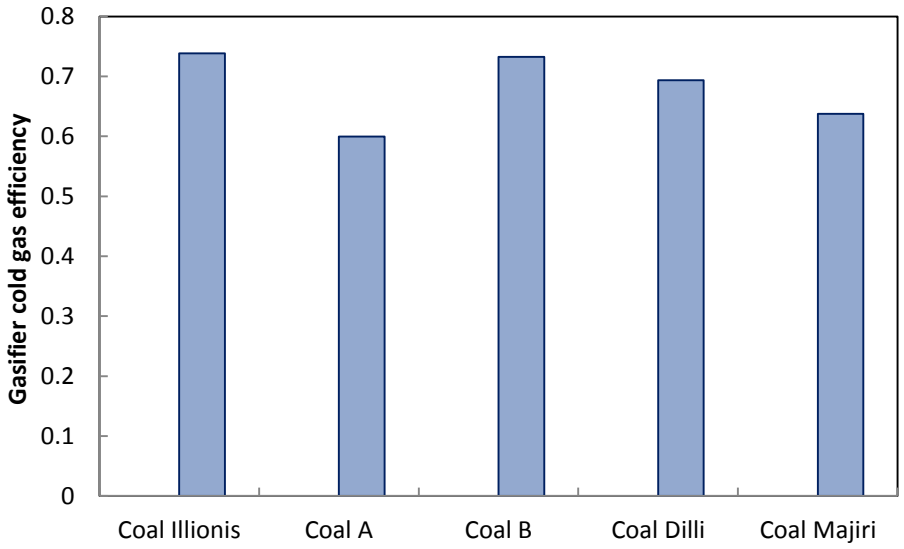

Figure 5.10: The effect of the coals on the gasifier cold gas efficiency

The variation of the hydrogen production for different types of coal is shown in Figure 5.11. For 108000 kg/hr input coal, the highest hydrogen production rate is estimated ~15730 kg/hr for Coal B, and the lowest ~7260 kg/hr for Coal Majiri. Thus, the weight ratio of the hydrogen yielded to the Coal B fed to this system is ~0.145 and ~0.067 for the coal Majiri fed. The main reason for that is hydrogen content in the coals. Coal B includes around ~5.6% hydrogen; however, hydrogen content in Coal Majiri is 3%. Although total hydrogen production is higher for the coals that include high amount of hydrogen and are high rankings, more hydrogen is obtained from the electrolyzer as shown in Figure 5.12 for low ranking coals. As mentioned before, different power consumers in the system such the ASU, multistage O_2 compressor, CO_2 removal and capturing units consume less power for low ranking coals, so more power is available to produce extra hydrogen from the electrolyzer. The rate of hydrogen production from the electrolyzer for Coal Majiri is ~720 kg/hr, which is ~10% of the total hydrogen production in this system. On the other hand, only ~3.2% of the total hydrogen production is obtained from the electrolyzer for Coal B. This means that a combined system to produce hydrogen can be a good option for production of hydrogen from the low ranking coals. In particular, hydrogen production rate that is produced from the electrolyzer will be higher if a high temperature steam electrolyzer is used instead of the alkaline water electrolyzer. Figure 5.13 shows hydrogen production rates using different types of coals from the PSA. As seen in the Figure, the majority of the hydrogen is produced from the PSA. It is also seen from the figure that there is significant difference in the production of hydrogen from the PSA for different types of coals. Hydrogen production from the PSA is estimated ~15200 kg/hr and 13000 kg/hr, respectively for Coal B and Coal

Illinois; however, this amount is around 6400 kg/hr and 6500 kg/hr, respectively for Coal A and Coal Majiri.

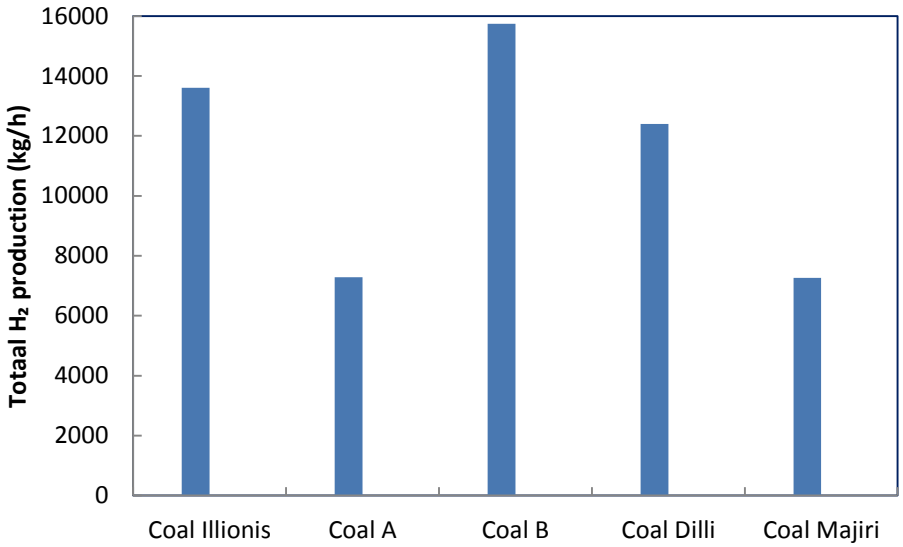

Figure 5.11: Variation of hydrogen production rate with different coal types

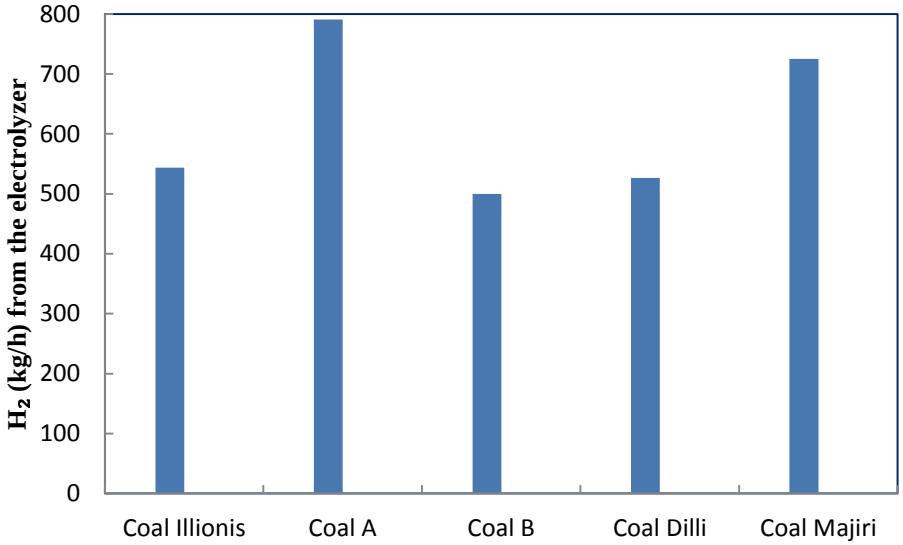

Figure 5.12: Variation of hydrogen production rate in the electrolyzer with different coal types

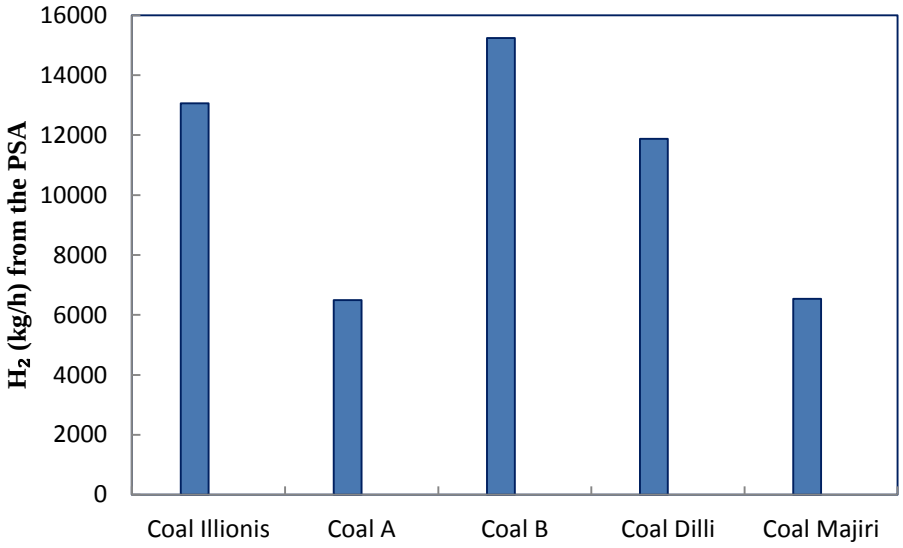

Figure 5.13: Variation of hydrogen production rate in the PSA with different coal types

A parametric study was conducted to estimate the effect of the H_2 recovery in the PSA unit on the rate of hydrogen production for the coals in the system. The hydrogen recovery was assumed between 0.7 and 0.9 for Coal Dilli, Coal B, and Coal Illinois. On the other hand, the H_2 recovery in the PSA was assumed between 0.7 and 0.8 for Coal A and Coal Majiri because the requirement power for the power consumer components in the system was not produced for the hydrogen recovery over 0.8 for these coals. Figure 5.14 shows the hydrogen production from the electrolyzer with changing hydrogen recovery in the PSA unit. As seen in the figure, there is no important increase on hydrogen production from the electrolyzer for Coal A and Coal Majiri for the variation of hydrogen recovery in the PSA. Increase of the H_2 production from the electrolyzer is only ~14% and ~13%, respectively for Coal A and Coal Majiri for the variation of H_2 recovery from 0.8 to 0.7. However, increase of the hydrogen production rate is estimated ~284%, ~151%, and ~190%,

respectively for Coal Dilli, Coal B, and Coal Illinois in the range of hydrogen recovery from 0.9 to 0.7. Although there is significant increase on hydrogen production from the electrolyzer for these coals, the total hydrogen production decreases as shown in Figure 5.15 due to lower H_2 recovery from the PSA. Total hydrogen production for Coal Majiri and Coal A is very close, so their hydrogen productions are shown in the figure as one line. For higher hydrogen recovery in the PSA, total hydrogen production in the system increases dramatically. For 0.9 H_2 recovery in the PSA unit, the weight ratio of the hydrogen yielded to the Coal B fed to this system is ~0.152 and the ratio to the Coal Illinois fed ~0.131. Thus, high H_2 recovery in the PSA seems better option to produce high amount of H_2 production rate.

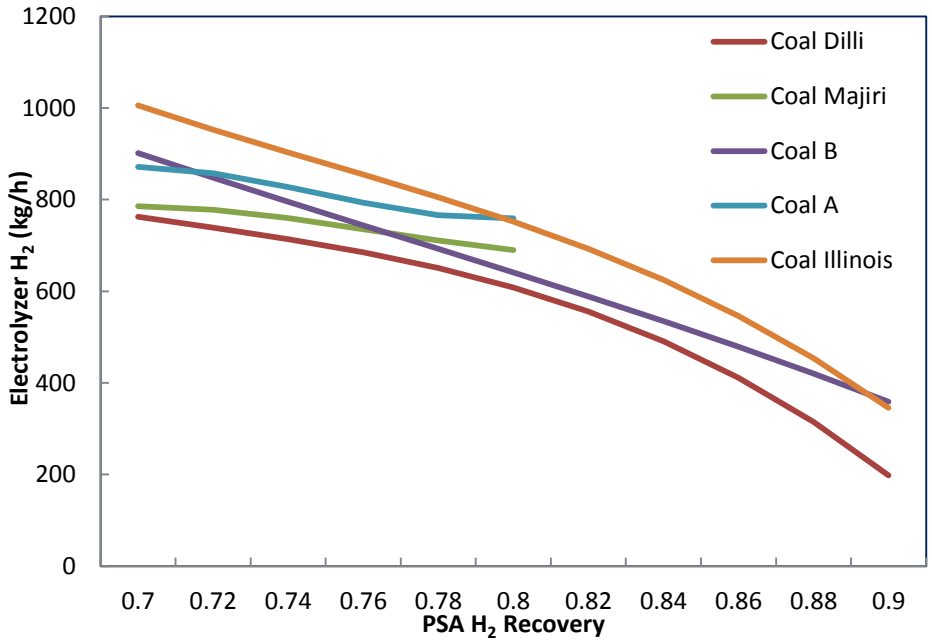

Figure 5.14: The effect of hydrogen recovery in the PSA on hydrogen production from the electrolyzer for different coals

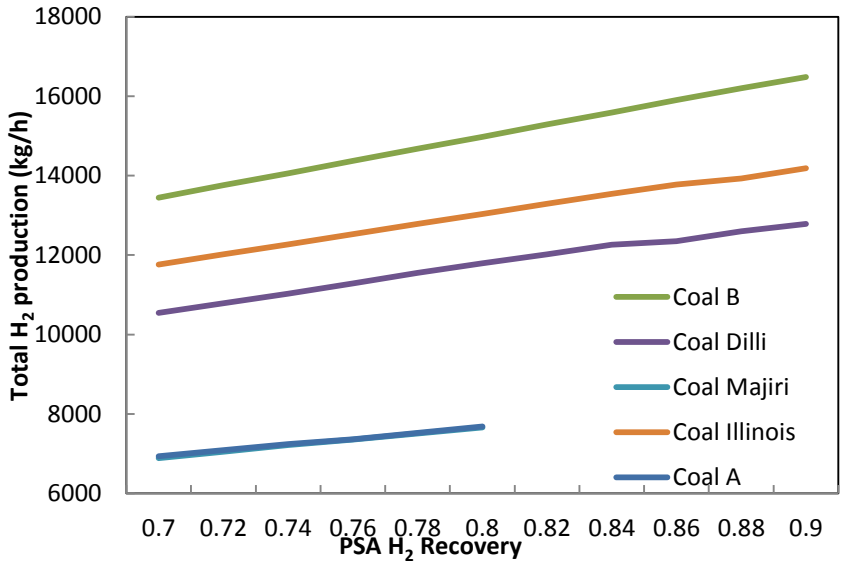

Figure 5.15: The effect of hydrogen recovery in the PSA on the total hydrogen production for different coals

Chapter 6
Conclusions and Recommendations

The present study shows that the combined coal gasification system and alkaline water electrolyzer allows for the production of large amounts of hydrogen with minimum emission.

The main findings of this study are listed as follows:

- The overall energy and exergy efficiencies of the system are ~58% and ~55%, respectively for Illinois#6 coal.
- The weight ratio of the hydrogen can be increased to ~0.131 if the hydrogen recovery in the PSA unit increases to 0.9 for Illinois#6 coal.
- Although the weight ratio of the hydrogen yielded is high for high ranking coals, this ratio decreases for low ranking coals. For example, the weight ratio of the hydrogen yielded to the Coal B fed to this system is ~0.145; however, it is ~0.067 for the Coal Majiri fed.
- The hydrogen production from the electrolyzer is much lower than hydrogen production from the PSA unit for high ranking coals.
- The hydrogen production from the electrolyzer is ~10% of the total hydrogen production for Coal Majiri in this system; however, it is only ~3.2% of the total hydrogen production for Coal B. Thus, a combined system may be more beneficial for low ranking coals.
- The most important power consumer is the ASU in the system for all of the coal types as shown in the results. However, there is a significant difference for power

production of the ASU for different types of coals because requirement of the oxygen for the gasification change with the coal types.

To develop this system, commercially available technology was only employed; however, alternative technologies can be used for future systems. Moreover, PSA unit can be removed, and hydrogen can be produced using only alkaline water electrolyzer. In this way, different coal types that include relatively less hydrogen may be evaluated to produce hydrogen.

In this study, we focus on performance of the system; however, the system can be modified using different technologies such as ionic transport membranes instead of the air separation unit, extensive economic analysis and life cycle assessment of the system should be investigated, and strong mathematical models should be constructed for performing experimental studies for the analysis and eventual benefits of the system. These strong mathematical equations would allow for obtaining more reliable results, and increasing flexibility of the system analysis. In particular, this would reveal the effects of different parameters on the system, and it could be analyzed more easily and accurately.

Appendix A

Properties of the Coals

Table A.1: Properties of Coal-A and Coal-B [81]

Coals	**A**	**B**
Proxanal		
FC	26,674	45.03
VM	39.3	44.168
MC	7.4	7.4
Ash	34.02	10.799
Ultanal		
Ash	34.02	10.799
Carbon	42.557	75.107
Hydrogen	4.233	5.4197
Oxygen	12.866	3.925
Nitrogen	1.452	2.944
Sulfur	4.8825	1.6056
Chlorine	0	0
Sulfanal		
Pyritic	1.539	0.71
Sulfate	1.3585	0.1356
Organic	1.985	0.76

Table A.2: Properties of Coal-Dilli and Coal-Majiri [82]

Coals	**Dilli**	**Majiri**
Proxanal		
MC	5.5	7.7
Ash	9.2	32.4
V.M	41.1	23.9
F.C	44.2	36.0
C.V (kcal/kg)	6350	4400
Ultanal		
Carbon	63.80	44.60
Hydrogen	4.80	3.00
Nitrogen	1.12	1.00
Sulfur	3.21	0.67
Sulfanal		
Pyrite	0.15	0.18
Sulfate	0.49	0.09
Organic	3.57	0.40

Bibliography

[1] Exxon Mobil. The outlook for energy: A view to 2040, 2013. Website: http://www.exxonmobil.com/corporate/files/news_pub_eo.pdf [accessed 20.09.13].

[2] Smalley RE. Future global energy prosperity: the terawatt challenge. Mrs Bull 2005; 30(6):412-417.

[3] EIA-U.S. Energy Information Administration. International energy outlook 2013, July 2013. Website: http://www.eia.gov/forecasts/ieo/pdf/0484(2013).pdf [accessed 20.09.13].

[4] National Renewable Energy Laboratory. A comparative review of a dozen national energy plans: Focus on renewable and efficient energy, March 2009. Website: http://www.nrel.gov/docs/fy09osti/4546.pdf [accessed 21.09.13].

[5] Parsons Brinckerhoff. Powering the future: Mapping our low-carbon path to 2050, December 2009. Website:http://www.pbworld.com/pdfs/powering_the_future/pbptf_full_report_pdf [accessed 21.09.13].

[6] The University of Melbourne Energy Research Institute. Australian sustainable energy: Zero carbon Australia stationary energy plan, 2010. Website:http://media.bze.org.au/ZCA2020_Stationary_Energy_Report_v1.pdf [accessed 21.09.13].

[7] European Climate Foundation (ECF). Roadmap2050: A practical guide to a prosperous low-carbon Europe, April 2010. Website: http://www.roadmap2050.eu/attachments/files/volume1_fullreport_PressPack.pdf [accessed 21.09.13].

[8] European Renewable Energy Council (EREC). Re-thinking 2050: A 100% renewable energy vision for the European Union, April 2010.Website:http://www.rethinking2050.eu [accessed 21.09.13].

[9] Jacobson MZ, Delucchi MA. Providing all global energy with wind, water, and solar power, Part I: Technologies, energy resources, quantities and areas of infrastructure, and materials. Energy Policy 2011; 39.1154-1169.

[10] Trainer T. 100% renewable supply? Comments on the reply by Jacobson and Delucchi to the critique by Trainer. Energy Policy 2013, 57: 634-640.

[11] U.S. Energy Information Administration. International Energy Outlook 2011, U.S. DOE, Washington, D.C., 2011.

[12] Organization of the Petroleum Exporting Countries. World Oil Outlook 2012, OPEC Secretariat, Vienna, 2012.

[13] Matsuo Y, Yaragisawa A, Yamashita Y. A global energy outlook to 2035 with strategic considerations for Asia and Middle East energy supply and demand interdependencies. Energy Strategy Reviews 2013; 2: 79-91.

[14] World Coal Association. Where is coal found? Website: http://www.worldcoal.org [accessed 11.04.13].

[15] Kothari R, Buddhi D, Sawhney RL. Comparison of environmental and economic aspects of various hydrogen production methods. Renewable&Sustainable Energy Reviews 2008; 12: 553-563.

[16] Dincer I. Green methods for hydrogen production. International Journal of Hydrogen Energy 2012; 37: 1954-1971.

[17] Demirci UB, Miele P. Overview of the relative greenness of the main hydrogen production processes. Journal of Cleaner Production 2013; 52: 1-10.

[18] Holladay JD, King DL, Wang Y. An overview of hydrogen production technologies. Catalysis Today 2009; 133: 244-260.

[19] Muradov NZ, Veziroglu TN. "Green" path from fossil-based to hydrogen economy: An overview of carbon-neutral technologies. International Journal of Hydrogen Energy 2008; 33: 6804-6839.

[20] Chaubey R, Sahu S, James OO, Maity S. A review on development of industrial processes and emerging techniques for production of hydrogen from renewable and sustainable sources. Renewable and Sustainable Energy Reviews 2013; 23: 443-462.

[21] Liu K, Chunshan S, Subramani V. Hydrogen and syngas production and purification technologies. AIChE, Wiley; 2010.

[22] Liu RS, Zhang L, Xuelieng S, Liu H, Zhang J. Electrochemical technologies for energy storage and conversion. Wiley-VCH; Volume 2, 2010.

[23] Wang ZL, Naterer GF, Gabriel KS, Gravelsins R, Daggupati VN. Comparison of sulfur-iodine and copper-chlorine thermochemical hydrogen production cycles. International Journal of Hydrogen Energy 2010; 35: 4820-4830.

[24] Lipman T. An overview of hydrogen production and storage systems with renewable hydrogen case studies. Clean Energy States Alliance, May 2011. Website: http://www.cleanenergystates.org [accessed 21.09.13].

[25] The Freedonia Group. World Hydrogen: Industry study with forecasts for 2016&2021, July 2012. Website: http://www.freedoniagroup.com [accessed 21.09.13].

[26] Bhattacharya D, Turton R, Zitney SE. Steady-state simulation and optimization of an integrated gasification combined cycle power plant with CO_2 capture. Industrial&Engineering Chemistry Research 2011; 50: 1674-1690.

[27] Botros BB, Brisson JG. Improving high temperature heat capture for power generation in gasification plants. International Journal of Heat and Mass Transfer 2013, 61, 129-137.

[28] Botero C, Randall PF, Robert DB, Howard JH, Ahmed FG. Performance of an IGCC Plant with Carbon Capture and Coal-CO_2-Slurry Feed: Impact of Coal Rank, Slurry Loading, and Syngas Cooling Technology. Industrial & Engineering Chemistry Research 2012: 51(36):11778-11790.

[29] Adams TA, Barton PI. High-efficiency power production from coal with carbon capture. AIChE Journal 2010; 50(12): 3120-3136.

[30] Siefert NS, Shawn L. Exergy and economic analyses of advanced IGCC–CCS and IGFC–CCS power plants. Applied Energy 2013; 107: 315-328.

[31] Li F, Zeng L, Fan LS. Techno-Economic Analysis of Coal-Based Hydrogen and Electricity Cogeneration Processes with CO_2 Capture. Industrial & Engineering Chemistry Research 2010; 49: 11018-11028.

[32] Ghosh S, De S. Exergy analysis of a cogeneration plant using coal gasification and solid oxide fuel cell. International journal of energy research 2006; 30: 647-658.

[33] Chen Y, Adams TA, Barton PI. Optimal design and operation of static energy polygeneration systems. Industrial&Engineering Chemistry Research 2010; 50: 5099-5113.

[34] Adams TA, Barton PI. Combining coal gasification and natural gas reforming for efficient polygeneration. Fuel Processing Technology 2011; 92: 639-655.

[35] Chiesa P, Consonni S, Kreutz T, Williams R. Co-production of hydrogen, electricity and CO_2 from coal with commercially ready technology. Part A: Performance and emissions. International Journal of Hydrogen Energy 2005; 30:747-767.

[36] Kreutz T, Williams R, Consonni S, Chiesa P. Co-production of hydrogen, electricity and CO_2 from coal with commercially ready technology. Part B: Economic analysis. International Journal of Hydrogen Energy 2005; 30: 769-784.

[37] Xu T, Zang G, Chen H, Dou B, Tan C. Co-production system of hydrogen and electricity based on coal partial gasification with CO_2 capture. International Journal of Hydrogen Energy 2012; 37: 11805-11814.

[38] Liszka M, Tomasz M, Manfrida G. Energy and exergy analysis of hydrogen-oriented coal gasification with CO_2 capture. Energy 2012; 45: 142-150.

[39] Cormos CC, Starr F, Tzimas E, Peteves S. Innovative concepts for hydrogen production processes based on coal gasification with CO_2 capture. International Journal of Hydrogen Energy 2008; 33: 1286-1294.

[40] Major environmental aspects of gasification-based power generation technologies final report. Website: http://www.netl.doe.gov/technologies/coalpower/gasification/pubs/pdf/final%20env.pdf [accessed 30.12.12].

[41] National Energy Laboratory (NETL). Gasifier: Commercial gasifiers: Entrained flow gasifiers, Shell Gasifier. Website:http://www.netl.doe.gov/technologies/coalpower/gasification/gasifipedia/shell [accessed 30.12.12].

[42] National Energy Laboratory (NETL). Gasifier: Commercial gasifiers: Entrained flow gasifiers, GE Energy Gasifier. Website:http://www.netl.doe.gov/technologies/coalpower/gasification/gasifipedia/ge.html [accessed 30.12.12].

[43] Rubin ES, Berkenpas M, Frey HC, Chen C, McCoy S, Zeremsky CJ. Development and application of optimal design capability for coal gasification systems. Pittsburg, US: Carnegie Mellon University: 2007.

[44] Different types of gasifiers and their integration with gas turbines. Website: http://www.netl.doe.gov/technologies/coalpower/turbines/refshelf/handbook/1.2.1.pdf [accessed 25.11.12].

[45] Wang Z, Yang J, Li Z, Xiang Y. Syngas composition study. Frontiers of Energy and Power Engineering in China 2009; 3: 369-372.

[46] Dugstad T. CO_2 capture from coal fired power plants. Master Thesis, Norwegian University of Science and Technology, June 2008.

[47] Kerry FG. Industrial gas handbook: Gas separation and purification. CRC Press, Taylor&Francis Group, 2006.

[48] NETL. Evaluation of alternate water gas shift configurations for IGCC systems, August 2009. Website:http://www.netl.doe.gov [accessed 25.11.12].

[49] Callaghan CA. Kinetics and catalysis of the water-gas-shift reaction: A microkinetic and graph theoretic approach. PhD diss., Worcester Polytechnic Institute, 2006.

[50] Mondal P, Dang GS, Garg MO. Syngas production through gasification and cleanup for downstream applications—Recent developments. Fuel Processing Technology 2011; 92(8): 1395-1410.

[51] Doctor RD, Molberg JC, Thimmapuram PR. KRW oxygen – blown gasification combined cycle: carbon dioxide recovery, transport, and disposal. Argonne National Laboratory 1996; ANL/ESD -34.

[52] Chen C. A technical and economic assessment of CO_2 captures technology for IGCC power plants. PhD diss., Carnegie Mellon University, 2005.

[53] Higman C, van der Burght M. Gasification. New York: Elsevier; 2003.

[54] Stocker J, Whysall M, Miller GQ. 30 years of PSA technology for hydrogen purification; UOP: Antwerp, Belgium, and Des Plaines, II, 1998.

[55] Ivy J. Summary of electrolytic hydrogen production. National Renewable Energy Laboratory; September 2004. NREL/MP-560-36734.

[56] Zeng K, Zhang D. Recent progress in alkaline water electrolysis for hydrogen production and applications. Progress in Energy and Combustion Science 2010; 36: 307-326.

[57] Dingizian A, Hanssan J, Persson T, Ekbarg H, Tuna P. A feasibility study on integrated hydrogen production. Lund Institute of Technology, 2007.

[58] AspenTech. Aspen Plus v7.3, 2011.

[59] Perna A. Combined power and hydrogen production from coal. Part A – Analysis of IGHP plants. International Journal of Hydrogen Energy 2008; 33: 2957 – 64.

[60] Prakash K. Simulation and optimization of hot syngas separation process in integrated gasification combined cycle. Master`s thesis, Massachusetts Institute of Technology, 2009.

[61] Field RP, Brasington R. Baseline Flowsheet Model for IGCC with Carbon Capture. Industrial & Engineering Chemistry Research 2011; 50(19); 11306-11312.

[62] Fan LS. Chemical looping systems for fossil energy conversion. Wiley-AIChE, 2011.

[63] Electric Power Research Institute. Coal Gasification Guidebook: Status, Applications, and Technologies: TR-102034, Research Project 2221-39, Final Report 1993.

[64] Frey HC, Akunuri N. Development and application of optimal design capability for coal gasification systems: Performance, emissions, and cost of Texaco gasifier – based systems using Aspen. Technical Report, Carnegie Mellon University, January 2001.

[65] Chen Y. Optimal design and operation of energy polygeneration systems. PhD diss., Massachusetts Institute of Technology, 2013.

[66] Gazzani M, Macchi E, Manzolini G. CO_2 capture in integrated gasification combined cycle with SEWGS-Part A: Thermodynamic performances. Fuel 2013; 105: 206-219.

[67] Hong J, Chaudhry G, Brisson JG, Field R, Gazzino M, Ghoniem AF. Analysis of oxy – fuel combustion power cycle utilizing a pressurized coal combustor. Energy 2009; 34: 1332 – 40.

[68] Aspen Plus v7.1. Getting started modeling processes with solids, 2009.

[69] Alie CF. CO_2 capture with MEA: Integrating the absorption process and steam cycle of an existing coal-fired power plant. Master`s Thesis, University of Waterloo, 2004.

[70] AspenTech. Aspen Plus model of CO_2 capture process by DEPG, 2011.

[71] Emun F, Gadalla M, Majozi T, Boer D. Integrated gasification combined cycle (IGCC) process simulation and optimization. Computers and Chemical Engineering 2010; 34: 331- 338.

[72] Bockelie, M. J., Denison, M. K., Chen, Z., Senior, C. L., & Sarofim, A. F. Using models to select operating conditions for gasifiers. Website: http://www.reactioneng.com/downloads/REI_processmodel.pdf [accessed 10.05.13].

[73] Bakshi BR, Timothy GG, Dusan PS. Thermodynamics and the destruction of the resources. Cambridge University Press, 2011.

[74] El – Emam RS, Dincer I, Naterer GF. Energy and exergy analyses of an integrated SOFC and coal gasification system. International Journal of Hydrogen Energy 2012; 37: 1689-1697.

[75] Al – Sulaiman FA. Thermodynamic modeling and thermoeconomic optimization of integrated trigeneration plants using Organic Rankine Cycles. PhD diss., University of Waterloo, 2010.

[76] Dincer I, Rosen MA. Exergy: energy, environment and sustainable development. 1st edition, Elsevier Science, 2007.

[77] Kanoglu M, Bolatturk A, Yilmaz C. Thermodynamic analysis of models used in hydrogen production by geothermal energy. International Journal of Hydrogen Energy 2010; 35: 8783 – 91.

[78] Yilmaz C, Kanoglu M, Bolatturk A, Gadalla M. Economics of hydrogen production and liquefaction by geothermal energy. International Journal of Hydrogen Energy 2012; 37: 2058 – 69.

[79] Wilcox J. Carbon capture. Springer, 2012.

[80] Bejan A, Tsatsaronis G, Moran M. Thermal design & Optimization.Wiley, 1996.

[81] Ramazan N, Ashraf A, Usman J, Shabbir S. et al. Modeling and simulation of coal gasification plant. Journal of Pakistan Institute of Chemical Engineers 2010; 38(1):32-38.

[82] Srivastava SK. Recovery of sulphur from very high ash fuel and fine distributed pyritic sulphur containing coal using ferric sulphate. Fuel Processing Technology 2003; 84: 37-46.